



NRL/MR/6110--11-9366

2010 ESTCP UXO Classification Study
Rougemont, NC
ESTCP MR-1034
Demonstration Data Report
Former Camp Butner
MTADS Discrimination Array (TEMTADS) Survey

NAGI KHADR
JAMES B. KINGDON
SAIC, Inc. - ASAD
Arlington, Virginia

GLENN R. HARBAUGH
DANIEL A. STEINHURST
Nova Research, Inc.
Alexandria, Virginia

October 20, 2011

Approved for public release; distribution is unlimited.

This page intentionally left blank.

Contents

Figures.....	viii
Tables.....	ix
Acronyms.....	xi
1.0 Introduction.....	1
1.1 Organization of this document.....	1
1.2 Study Background and Objectives.....	1
1.3 Specific Objectives of Demonstration	1
2.0 Technology	1
2.1 Technology Description.....	1
2.1.1 EMI Sensors.....	1
2.1.2 Sensor Array	5
2.1.3 Application of the Technology	9
2.1.4 Development of the Technology.....	9
2.2 Advantages and Limitations of the Technology	10
3.0 Performance Objectives	11
3.1 Objective: Site Coverage	11
3.1.1 Metric.....	11
3.1.2 Data Requirements.....	11
3.1.3 Success Criteria.....	11
3.2 Objective: Instrument Verification Strip Results.....	11
3.2.1 Metric.....	11
3.2.2 Data Requirements.....	11
3.2.3 Success Criteria.....	12

3.3	Objective: Location Accuracy	13
3.3.1	Metric	13
3.3.2	Data Requirements.....	13
3.3.3	Success Criteria.....	13
3.4	Objective: Depth Accuracy.....	13
3.4.1	Metric	13
3.4.2	Data Requirements.....	13
3.4.3	Success Criteria.....	13
3.5	Objective: Production Rate	14
3.5.1	Metric	14
3.5.2	Data Requirements.....	14
3.5.3	Success Criteria.....	14
3.6	Objective: Data Throughput	14
3.6.1	Metric	14
3.6.2	Data Requirements.....	14
3.6.3	Success Criteria.....	14
3.7	Objective: Reliability and Robustness.....	15
3.7.1	Data Requirements.....	15
4.0	Site Description.....	15
5.0	Test Design	15
5.1	Conceptual Experimental Design	15
5.2	Site Preparation.....	15
5.3	Systems Specification	15
5.3.1	MTADS Tow Vehicle.....	16

5.3.2	RTK GPS System	16
5.3.3	Time-Domain Electromagnetic Sensor.....	17
5.4	Calibration Activities	17
5.4.1	Background Data	18
5.4.2	Instrument Verification Strip Data.....	21
5.5	Data Collection Procedures.....	23
5.5.1	Scale of Demonstration.....	23
5.5.2	Sample Density	24
5.5.3	Quality Checks.....	24
5.5.4	Data Handling	25
5.6	Validation.....	26
6.0	Data Analysis Plan.....	26
6.1	Preprocessing	26
6.2	Parameter Estimation	27
6.3	Data Product Specifications	28
7.0	Performance Assessment	29
7.1	Objective: Site Coverage	29
7.1.1	Metric.....	29
7.1.2	Data Requirements.....	29
7.1.3	Success Criteria.....	29
7.1.4	Results.....	29
7.2	Objective: Instrument Verification Strip Results.....	29
7.2.1	Metric.....	29
7.2.2	Data Requirements.....	29

7.2.3	Success Criteria.....	30
7.2.4	Results.....	31
7.3	Objective: Location Accuracy	31
7.3.1	Metric.....	31
7.3.2	Data Requirements.....	31
7.3.3	Success Criteria.....	31
7.3.4	Results.....	31
7.4	Objective: Depth Accuracy.....	31
7.4.1	Metric.....	32
7.4.2	Data Requirements.....	32
7.4.3	Success Criteria.....	32
7.4.4	Results.....	32
7.5	Objective: Production Rate.....	32
7.5.1	Metric.....	32
7.5.2	Data Requirements.....	32
7.5.3	Success Criteria.....	32
7.5.4	Results.....	32
7.6	Objective: Data Throughput	33
7.6.1	Metric.....	33
7.6.2	Data Requirements.....	33
7.6.3	Success Criteria.....	33
7.6.4	Success Criteria.....	33
7.7	Objective: Reliability and Robustness.....	33
7.7.1	Data Requirements.....	34

7.7.2	Results.....	34
8.0	References.....	35
Appendix A.	Points of Contact.....	37
Appendix B.	Data Formats.....	39
B.1	Position / orientation data file (*.GPS).....	39
B.2	TEM Data file (*.TEM).....	39
B.3	Anomaly Parameter Output file.....	40
B.4	README file.....	41

Figures

Figure 2-1 – Construction details of an individual EMI sensor (left panel) and the assembled sensor with end caps attached (right panel).	2
Figure 2-2 – Measured transmit current (on-time upper panel, off-time second panel), full measured signal decay (third panel), and gated decay (fourth panel) as discussed in the text.	3
Figure 2-3 – Measured response from a 2-in steel sphere placed 25 cm from the sensor. Decays 1, 1001, 2001, and 3001 from a series that started from a cold start are plotted along with the expected response from this target.	4
Figure 2-4 – Measured response from three calibration coils and the background response between measurements plotted on a semi-log plot to emphasize the exponential nature of the decay. The decay time constants extracted from the measurements are listed in the legend.	4
Figure 2-5 – Sketch of the EMI sensor array showing the position of the 25 sensors and the three GPS antennae.	5
Figure 2-6 – Sensor array mounted on the MTADS EMI sensor platform.	6
Figure 2-7 – Comparison of the response of the array members. The measured decay from a 2-in steel sphere held 30 cm below each sensor in turn is plotted. The decays are indistinguishable.	6
Figure 2-8 – The response of nine of the individual sensors to a 40-mm projectile located under the center of the array.	7
Figure 2-9 – Derived response coefficients for a 40-mm projectile using the measurements of which the decays shown in Figure 2-8 are a subset.	8
Figure 2-10 – Derived response coefficients from a cued measurement over "Cylinder E" in the test field.	8
Figure 2-11 – Three sets of β s derived from three measurements over a 4.2-in mortar baseplate at different position/orientation pairs.	9
Figure 5-1 – MTADS tow vehicle and magnetometer array.	16
Figure 5-2 – Locations of anomaly-free areas determined beforehand from the EM61 cart data.	19

Figure 5-3 – Intra- and inter- daily variations in the response of the TEMTADS to background anomaly-free areas through the duration of the demonstration at Camp Butner. The red points represent the average measured signal of the 25 monostatic quantities, while the bars represent the standard deviation of those quantities (i.e. 1σ about the mean).	20
Figure 5-4 – Derived response coefficients for item 1001 emplaced in the IVS (left panel) and amplitude variations at 0.042 ms in the derived response coefficients for all items emplaced in the IVS (right panel). β_1 is in red; β_2 is in green; and β_3 is in blue.	22
Figure 5-5 – Position errors for item 1001 emplaced in the IVS (left panel) and position error statistics for all items emplaced in the IVS (right panel). Easting data are in black and Northing data are in red.	23
Figure 5-6 – QC tool showing a contour plot of the monostatic signals at 0.042 ms for the 25 transmit/receive pairs (left panel) alongside a contour plot of a 5 m x 5 m area of the EM61 data centered about the array and showing all the anomalies that are on the list and within this area (right panel).	25
Figure 6-1 – Principal axis polarizabilities for a ½ cm thick by 25cm long by 15cm wide mortar fragment.	28

Tables

Table 3-1 – Performance Objectives for this Demonstration	12
Table 5-1 – Locations of Anomaly-Free Areas used for Background Measurements.	18
Table 5-2 – Summary of the Daily Variation in the Mean and Standard Deviation of the Signals Measured for the Background Areas.....	20
Table 5-3 – Details of Former Camp Butner IVS.....	21
Table 5-4 – Summary of the Amplitude Variations at 0.042 ms in the Derived Response Coefficients for All Items Emplaced in the IVS.....	21
Table 5-5 – Summary of Position and Depth Error Statistics for all items emplaced in the IVS.	23
Table 7-1 – Performance Results for this Demonstration.....	30

This page intentionally left blank.

Acronyms

Abbreviation	Definition
AMTADS	Airborne Multi-sensor Towed Array Detection System
APG	Aberdeen Proving Ground
ASCII	American Standard Code for Information Interchange
ATC	Aberdeen Test Center
CD-R	Compact Disk - Recordable
DAQ	Data Acquisition (System)
DAS	Data Analysis System
DVD-R	Writable digital versatile disc
EMI	Electro-Magnetic Induction
ESTCP	Environmental Security Technology Certification Program
FQ	Fix Quality
FUDS	Formerly -Used Defense Site
GPS	Global Positioning System
HASP	Health and Safety Plan
Hz	Hertz
IVS	Instrument Verification Strip
MM	Munitions Management
MTADS	Multi-sensor Towed Array Detection System
NMEA	National Marine Electronics Association
NRL	Naval Research Laboratory
Pd	Probability of Detection
POC	Point of Contact
(PTNL,)AVR	Time, Yaw, Tilt, Range for Moving Baseline RTK NMEA-0183 message
(PTNL,)GGK	Time, Position, Position Type, DOP NMEA-0183 message
QC	Quality Control
ROC	Receiver Operating Characteristic
RTK	Real Time Kinematic
Rx	Receiver
SAIC	Science Applications International Corporation
SERDP	Strategic Environmental Research and Development Program
SLO	San Luis Obispo
TEM	Time-domain Electro-Magnetic
TEMTADS	Time-domain Electro-Magnetic MTADS
Tx	Transmit(ter)

1.0 INTRODUCTION

1.1 ORGANIZATION OF THIS DOCUMENT

As part of the Environmental Security Technology Certification Program (ESTCP) UXO Classification Study at the former Camp Butner (Butner), NC, the Naval Research Laboratory (NRL) Multi-sensor Towed Array Detection System (MTADS) EMI Array for Cued Discrimination, or TEMTADS was demonstrated for cued data collection. The acquisition of these data as part of the Study demonstration in July 2010 is presented in this document. To limit the repetition of information, both the study and site specific information that is presented in the ESTCP UXO Classification Study Demonstration Plan [1] is noted and not repeated in this document.

1.2 STUDY BACKGROUND AND OBJECTIVES

Please refer to the 2010 ESTCP UXO Classification Study Demonstration Plan.

1.3 SPECIFIC OBJECTIVES OF DEMONSTRATION

As part of NRL's ESTCP-funded UXO Classification Study, Nova Research, Inc. and SAIC conducted a cued discrimination survey within the 10 acre final demonstration site at the former Camp Butner, NC FUDS of 2,304 previously-identified anomalies. This survey utilized the Naval Research Laboratory (NRL) TEMTADS. Characterization of the system responses to the items of interest were determined using measurements taken both off-site (in-air data taken prior to the demonstration effort) and on-site (mostly Instrument Verification Strip (IVS) data). These data were collected in accordance with the overall study objectives and demonstration plan. This document describes the TEMTADS data collection demonstration at the former Camp Butner.

2.0 TECHNOLOGY

2.1 TECHNOLOGY DESCRIPTION

2.1.1 EMI Sensors

The EMI sensor used in the TEMTADS array is based on the Navy-funded Advanced Ordnance Locator (AOL), developed by G&G Sciences. The AOL consists of three transmit coils arranged in a 1-m cube; we have adopted the transmit (Tx) and receive (Rx) subsystems of this sensor directly, converted to a 5 x 5 array of 35 cm square sensors, and made minor modifications to the control and data acquisition computer to make it compatible with our deployment scheme.

A photograph of an individual sensor element under construction is shown in the left panel of Figure 2-1. The transmit coil is wound around the outer portion of the form and is 35 cm on a side. The 25-cm receive coil is wound around the inner part of the form which is re-inserted into the outer portion. An assembled sensor with the top and bottom caps used to locate the sensor in the array is shown in the right panel of Figure 2-1.

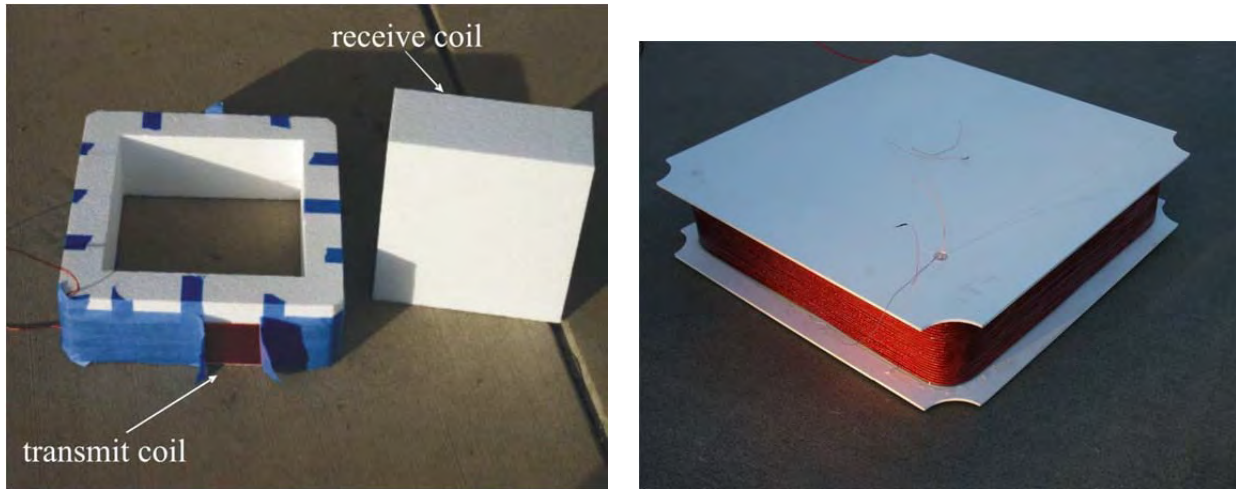


Figure 2-1 – Construction details of an individual EMI sensor (left panel) and the assembled sensor with end caps attached (right panel).

Decay data are collected with a 500 kHz sample rate until 25ms after turn off of the excitation pulse. This results in a raw decay of 12,500 points; too many to be used practically. These raw decay measurements are grouped into 115 logarithmically-spaced “gates” with center times ranging from 42 μ s to 24.35 ms with 5% widths and are saved to disk. Examples of the measured transmit pulse, raw decay, and gated decay are shown in Figure 2-2.

The individual sensors (consisting of transmit electronics, transmit and receive coils, pre-amp, and digitizer) were characterized at G & G Sciences before approval was given for construction of the array. Examples of the characterization data are shown in Figure 2-3 and Figure 2-4. System stability is demonstrated in Figure 2-3 which plots the normalized (by measured transmit current) response of a 2-in steel ball at a 25 cm separation from the sensor. The data plotted are decays 1, 1001, 2001, and 3001 in a continuously-triggered series that began from a cold start and ran for 2.5 hours. For comparison purposes, the expected response from this sphere is plotted in black. As can be seen, the sensor exhibits excellent stability which will be important for the cued deployment planned.

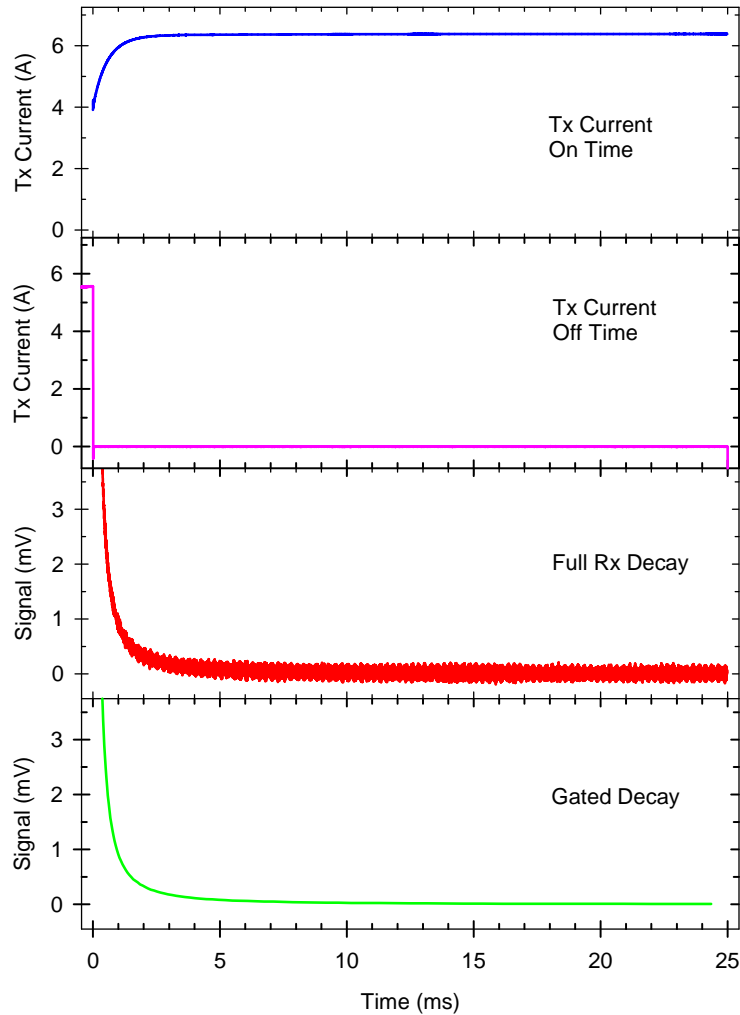


Figure 2-2 – Measured transmit current (on-time upper panel, off-time second panel), full measured signal decay (third panel), and gated decay (fourth panel) as discussed in the text.

The second important characterization test is sensor response linearity. Since we intended to collect decay data to late times and over several orders of magnitude in amplitude, the linearity of system response was very important. To characterize this property of the sensor, we constructed a series of copper coils with nominal decay time constants of 2, 4, and 6 ms. The responses of the three coils are shown in Figure 2-4 which plots the measured decays on a set of semi-log axes. After a transient at early times, the decays exhibit clean exponential behavior with measured decay times of 1.8, 3.3, and 5.8 ms. Careful calculation of the expected decay times at the temperature at which the tests were conducted results in expected values of 1.82, 3.26, and 5.73 ms; the measured values are in excellent agreement with these.

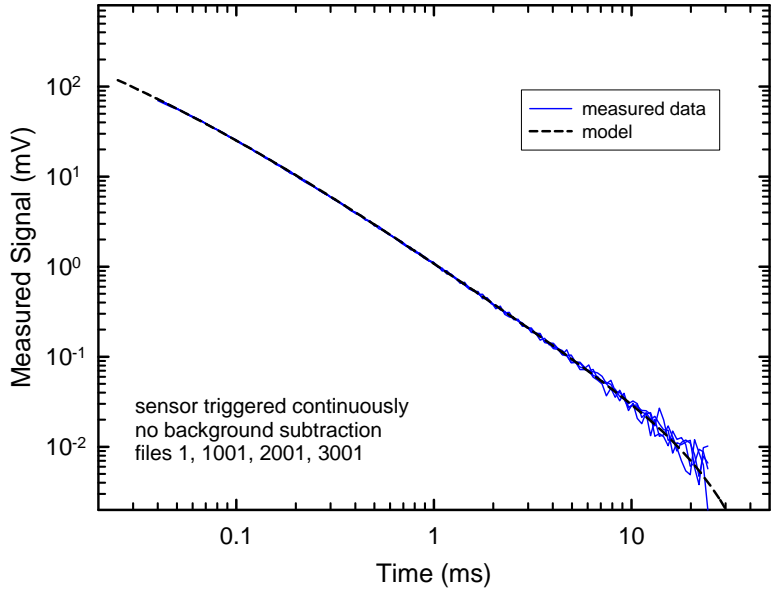


Figure 2-3 – Measured response from a 2-in steel sphere placed 25 cm from the sensor. Decays 1, 1001, 2001, and 3001 from a series that started from a cold start are plotted along with the expected response from this target.

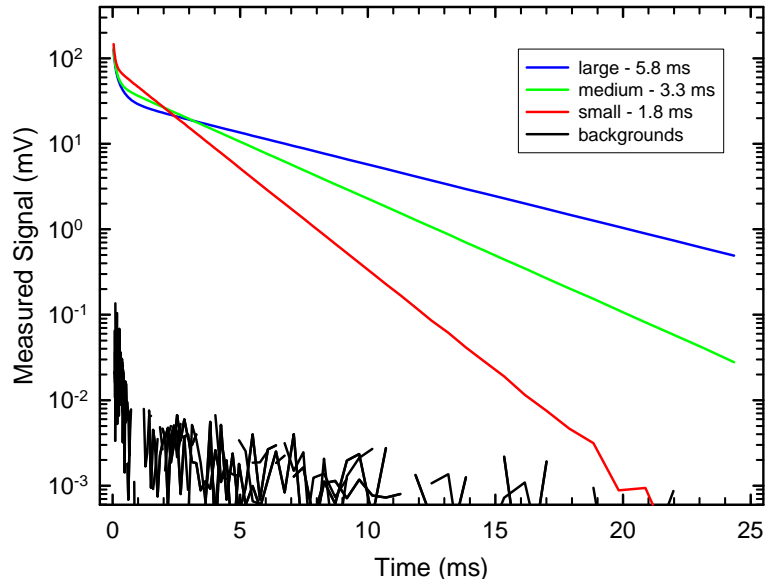


Figure 2-4 – Measured response from three calibration coils and the background response between measurements plotted on a semi-log plot to emphasize the exponential nature of the decay. The decay time constants extracted from the measurements are listed in the legend.

2.1.2 Sensor Array

The twenty-five individual sensors are arranged in a 5 x 5 array as shown in Figure 2-5. The center-to-center distance is 40 cm yielding a 2 m x 2 m array. Also shown in Figure 2-5 is the position of the three GPS antennae that are used to determine the location and orientation of the array for each cued measurement. A picture of the array mounted on the MTADS EMI sensor platform is shown in Figure 2-6.

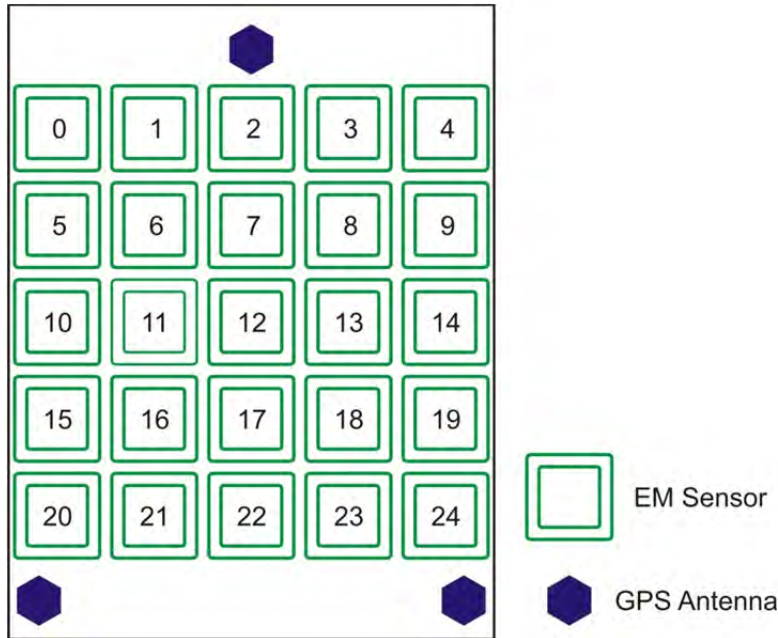


Figure 2-5 – Sketch of the EMI sensor array showing the position of the 25 sensors and the three GPS antennae.

After assembly of the array, a number of array calibration measurements were performed. The first task was to ensure that each of the individual sensors has equivalent response. A jig was constructed that allows us to mount a 2-in steel sphere 30 cm below each array element in turn. Data collected using this jig is shown in Figure 2-7. As can be seen, the measured decays from each of the sensors plotted are indistinguishable.

After this, the assembled array was used to measure the response of a number of inert ordnance items and stimulants both mounted on a test stand and mounted on the sensor platform in our test field. For each series of measurements with the full array, we cycle through the sensors transmitting from each in turn. After each excitation pulse, we record the response of all twenty-five receive coils. Thus, there are 625 (25 x 25) individual transmit/receive pairs recorded, making it difficult to present a full measurement in any coherent way. In Figure 2-8, we plot nine of the transmit/receive pairs resulting from excitation of a 40-mm projectile located under the center of the array. The decays plotted correspond to the signal received on the nine central

sensors (reference Figure 2-5 for the sensor numbering) when that sensor transmits. In other words, the results of nine individual monostatic measurements are presented.



Figure 2-6 – Sensor array mounted on the MTADS EMI sensor platform.

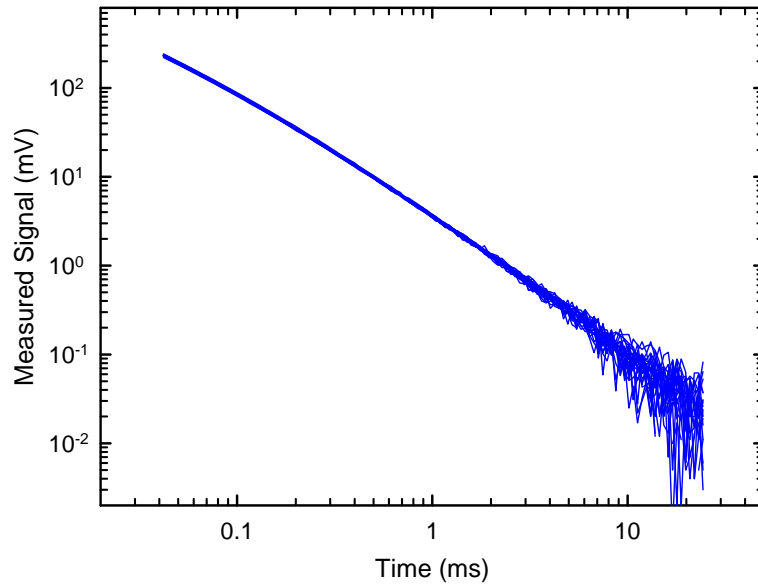


Figure 2-7 – Comparison of the response of the array members. The measured decay from a 2-in steel sphere held 30 cm below each sensor in turn is plotted. The decays are indistinguishable.

All 625 measurements are used for the inversion to recover target parameters. The inversion results for the decay data shown in Figure 2-8 are shown in Figure 2-9. As we expect for an object with axial symmetry such as a 40-mm projectile, we recover one large response coefficient and two equal, but smaller ones. These response coefficients will be the basis of the discrimination decisions in this demonstration. Derived β s for “Cylinder E” (3" x 12" steel cylinder) in the test field are shown for comparison in Figure 2-10.

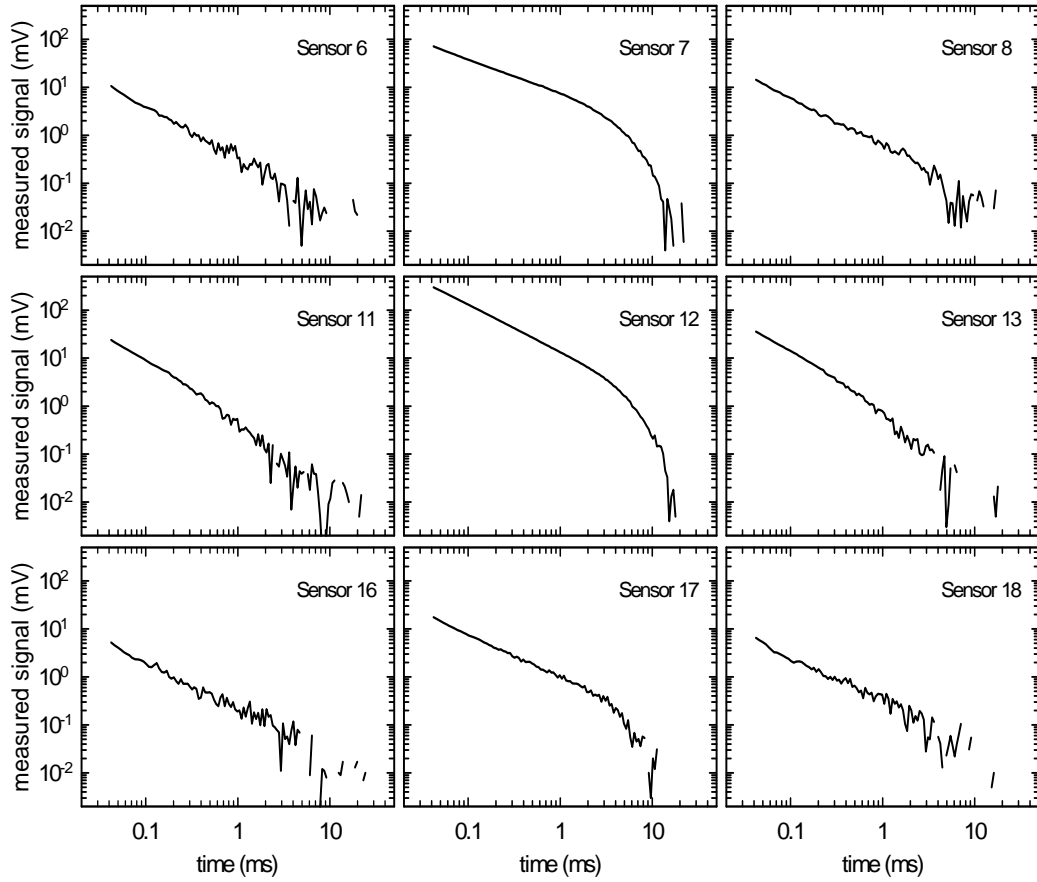


Figure 2-8 – The response of nine of the individual sensors to a 40-mm projectile located under the center of the array.

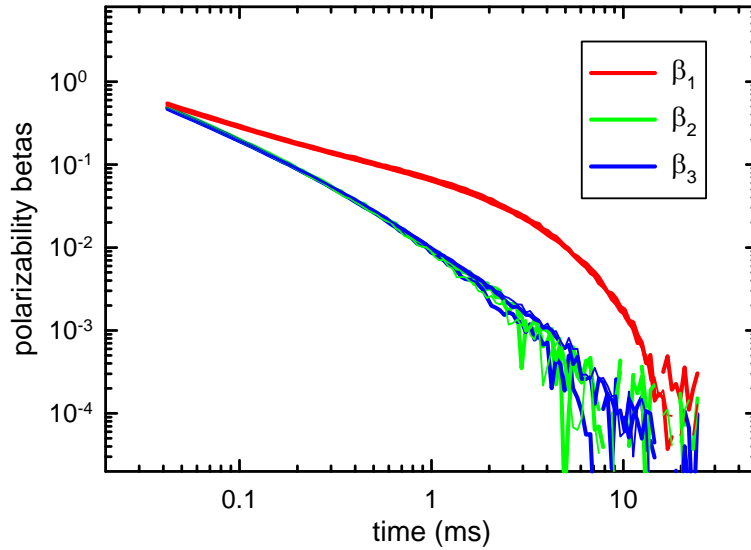


Figure 2-9 – Derived response coefficients for a 40-mm projectile using the measurements of which the decays shown in Figure 2-8 are a subset.

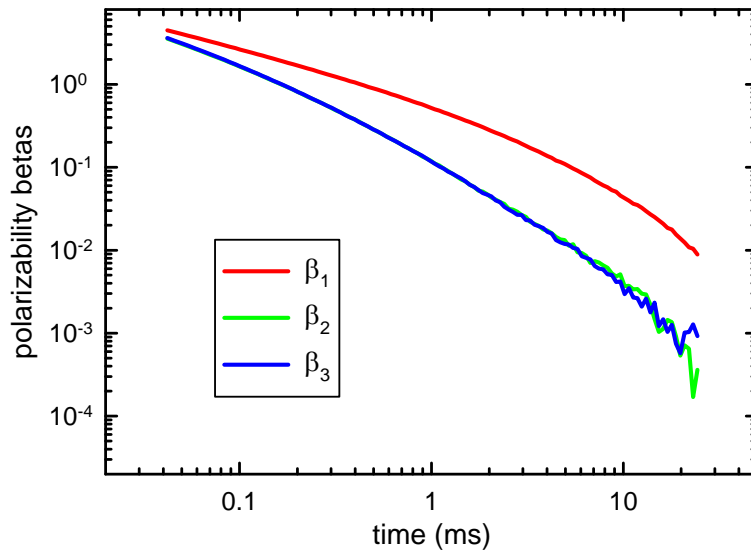


Figure 2-10 – Derived response coefficients from a cued measurement over "Cylinder E" in the test field.

The final array characterization test was to confirm that the response coefficients we recover are invariant to object position and orientation under the array. Figure 2-11 shows the derived β s plotted for a 4.2-in mortar baseplate after measurements at three position/orientation pairs. As can be seen, the inversion results are robust to variation in the objects position and orientation.

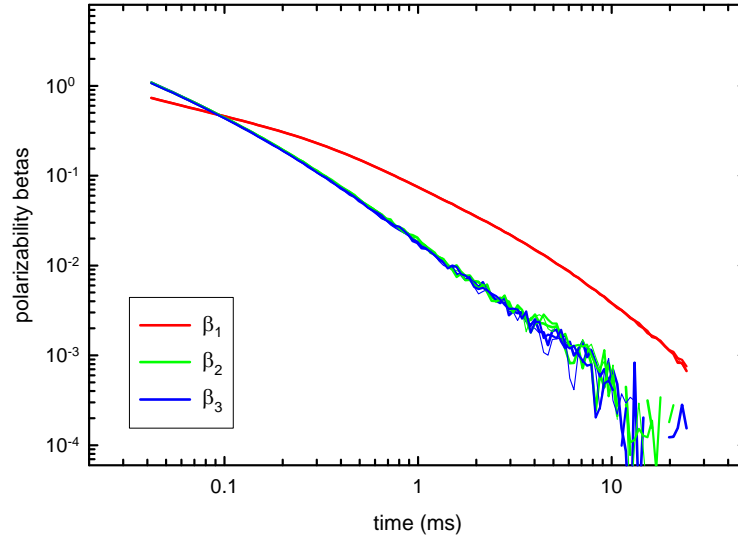


Figure 2-11 – Three sets of β s derived from three measurements over a 4.2-in mortar baseplate at different position/orientation pairs.

2.1.3 Application of the Technology

Application of this technology is straightforward. A list of target positions is developed from some source; in the case of this demonstration, the anomaly list was generated by the ESTCP Program Office using the EM61 MkII Cart data. A target file, containing the target location and an optional flag for additional ‘stacking’ or averaging, for each anomaly is transferred to the system control program which uses the information from the three GPS antennae to guide the operator to position the array over each target in turn. When positioned over the target, we step through the array sensors sequentially, just as in the characterization measurements discussed in the preceding section, and collect decay data from all twenty-five receive coils for each excitation. These data are then stored electronically on the data acquisition computer. Following the EMI data collection, a few seconds of platform position and orientation data are also collected to allow translation of the inverted target position, which is relative to the array, to absolute position and orientation. The EMI and position data are transferred to the analyst several times each day for near real-time quality control and analysis at the demonstration site.

2.1.4 Development of the Technology

The Chemistry Division of NRL has participated in several programs funded by SERDP and ESTCP whose goal has been to enhance the discrimination ability of MTADS for both magnetometer and EMI array configurations. The process was based on making use of both the location information inherent in an item’s magnetometry response and the shape and size information inherent in the response to the time-domain electromagnetic induction (EMI) sensors that are part of the baseline MTADS in either a cooperative or joint inversion. In these past efforts, our classification ability has been limited by the information available from the time-

domain EMI sensor. Further information regarding the MTADS magnetometer and EM61 sensor arrays can be found in Reference 2 and the references within.

To make further progress on UXO classification, a sensor with more available information was required. The Geophex, Ltd. GEM-3 sensor is a frequency-domain EMI sensor with up to ten transmit frequencies available for simultaneous measurement of the in-phase and quadrature response of the target. In principle, there is much more information available from a GEM-3 sensor for use in discrimination decisions. However, the commercial GEM-3 sensor is a hand-held instrument with relatively slow data rates and is thus not very amenable to rapid, wide area surveys. ESTCP Project MR-0033, Enhanced UXO Discrimination Using Frequency-Domain Electromagnetic Induction, was funded to overcome this limitation by integrating an array of GEM-3 sensors with the MTADS platform [3]. Further details can be found in References 2 and 3.

Reference 4 compares the detection-only performance of the magnetometer, the second-generation MTADS EM61 MkII, and the GEMTADS arrays to other demonstrators at both of the Standardized UXO Technology Demonstration Sites. All three sensor arrays were also demonstrated in the Spring of 2007 as part of the ESTCP UXO Discrimination Study at the former Camp Sibert [2]. The magnetometer and EM61 MkII sensor arrays were demonstrated in the Spring of 2009 as part of the ESTCP UXO Classification Study at the former Camp San Luis Obispo [5].

Under SERDP project MR-1315 (EMI Sensor Optimized for UXO Discrimination) and ESTCP project MR-0601, NRL, SAIC, and G&G Sciences have developed a time-domain EMI sensor optimized for the classification of UXO. The TEMTADS array was constructed in 2007 and field tested at the APG Standardized UXO Test Site in June 2008 [6,7]. After processing, ranked dig lists were generated and submitted to ATC for scoring. The results of the demonstration, as scored by ATC are available in Reference 6. The TEMTADS array was also demonstrated as part of the 2009 ESTCP UXO Classification Study at the former Camp San Luis Obispo [8]. The results of these demonstrations are discussed in the ESTCP Project Final Report [9].

2.2 ADVANTAGES AND LIMITATIONS OF THE TECHNOLOGY

The TEMTADS array is designed to combine the data advantages of a gridded survey with the coverage efficiencies of a vehicular system. We expect to collect data equal, if not better, in quality to the best gridded surveys (the relative position and orientation of the sensors will be better than gridded data) while prosecuting many more targets each field day.

There are obvious limitations to the use of this technology. The array is a 2-m square so fields where the vegetation or topography interferes with passage a trailer of that size will not be amenable to the use of the present array. The other serious limitation is anomaly density. For all sensors, there is a limiting anomaly density above which the response of individual targets cannot be separated. We have chosen relatively small sensors for this array which should help with this problem but we cannot eliminate it. Based on experiments at our test pit at Blossom Point, the results of the APG demonstration, and work done on the Camp Sibert data, anomaly

densities of 300 anomalies/acre or higher would limit the applicability of this system as more than 20% of the anomalies would have another anomaly within a meter.

3.0 PERFORMANCE OBJECTIVES

Performance objectives for the demonstration are given in Table 3-1 to provide a basis for evaluating the performance and costs of the demonstrated technology. Since this is a classification technology, the performance objectives focus on the second step of the UXO survey problem; we assume that the anomalies from all targets of interest have been detected and included on the target list provided to us.

3.1 OBJECTIVE: SITE COVERAGE

A list of previously identified anomalies was provided by the Program Office.

3.1.1 Metric

Site coverage is defined as the fraction of the assigned anomalies surveyed by the TEMTADS.

3.1.2 Data Requirements

The collected data are compared to the original anomaly list. All interferences are noted in the field log book.

3.1.3 Success Criteria

The objective is considered met if 100% of the assigned anomalies are surveyed with the exception of areas that cannot be surveyed due to topology / vegetation interferences.

3.2 OBJECTIVE: INSTRUMENT VERIFICATION STRIP RESULTS

This objective confirms that the sensor system is in good working order and collecting physically valid data each day. The IVS is to be surveyed twice daily. The amplitude of the derived response coefficients for each emplaced item is compared to the running average of the demonstration for reproducibility. The extracted fit location of each item is compared to the reported ground truth.

3.2.1 Metric

The reproducibility of the measured response of the sensor system to the emplaced items and of the extracted locations of the emplaced items defines this metric.

3.2.2 Data Requirements

The tabulated fit parameters for the data corresponding to each emplaced item in terms of derived response coefficients, location and depth.

Table 3-1 – Performance Objectives for this Demonstration

Performance Objective	Metric	Data Required	Success Criteria
Quantitative Performance Objectives			
Site Coverage	Fraction of assigned anomalies interrogated	Survey results	100% as allowed for by topography / vegetation
Instrument Verification Strip (IVS) Results	System responds consistently to emplaced items	Daily IVS data	<ul style="list-style-type: none"> • $\leq 15\%$ rms variation in β amplitude • Down-track location $\pm 25\text{cm}$
Location Accuracy	Average error and standard deviation in both axes for interrogated items	<ul style="list-style-type: none"> • Estimated location from analyses • Ground truth from validation effort 	ΔN and $\Delta E < 5 \text{ cm}$ σN and $\sigma E < 10 \text{ cm}$
Depth Accuracy	Standard deviation in depth for interrogated items	<ul style="list-style-type: none"> • Estimated location from analyses • Ground truth from validation effort 	$\Delta \text{Depth} < 5 \text{ cm}$ $\sigma \text{Depth} < 10 \text{ cm}$
Production Rate	Number of anomalies investigated each day	<ul style="list-style-type: none"> • Survey results • Log of field work 	125 anomalies/day
Data Throughput	Throughput of data QC process	Log of analysis work	All data QC'ed on site and at pace with survey
Qualitative Performance Objective			
Reliability and Robustness	General Observations	Team feedback and recording of emergent problems	Field team comes to work smiling

3.2.3 Success Criteria

The objective is considered met if the RMS amplitude variation of the derived response coefficients is less than 15% and the down-track fit location of the anomaly is within 25 cm of the stated location.

3.3 OBJECTIVE: LOCATION ACCURACY

An important measure of how efficiently any required remediation will proceed is the accuracy of predicted location of the targets marked to be dug. Large location errors lead to confusion among the UXO technicians assigned to the remediation costing time and often leading to removal of a small, shallow object when a larger, deeper object was the intended target.

3.3.1 Metric

The average error and standard deviation in both horizontal axes defines this metric.

3.3.2 Data Requirements

The anomaly fit parameters and the ground truth for the excavated items. Since these data are not available to us at this time, the IVS data are used to determine the performance of the fitting routines in terms of the location accuracy.

3.3.3 Success Criteria

This objective is considered met if the average error in position for both Easting and Northing quantities is less than 5 cm and the standard deviation for both is less than 10 cm.

3.4 OBJECTIVE: DEPTH ACCURACY

An important measure of how efficiently any required remediation will proceed is the accuracy of predicted depth of the targets marked to be dug. Large depth errors lead to confusion among the UXO technicians assigned to the remediation costing time and often leading to removal of a small, shallow object when a larger, deeper object was the intended target.

3.4.1 Metric

The standard deviation of the predicted depths with respect to the ground truth defines this metric.

3.4.2 Data Requirements

The anomaly fit parameters and the ground truth for the excavated items. Since these data are not available to us at this time, the IVS data are used to determine the performance of the fitting routines in terms of the depth accuracy.

3.4.3 Success Criteria

This objective is considered met if the average error in depth is less than 5 cm and the standard deviation is less than 10 cm.

3.5 OBJECTIVE: PRODUCTION RATE

This objective considers a major cost driver for the collection of high-density, high-quality geophysical data, the production rate. The faster quality data can be collected, the higher the financial return on the data collection effort.

3.5.1 Metric

The number of anomalies investigated per day determines the production rate for a cued survey system.

3.5.2 Data Requirements

The metric can be determined from the combination of the field logs and the survey results. The field logs require the amount of time per day spent acquiring the data and the survey results determine the number of anomalies investigated in that time period.

3.5.3 Success Criteria

This objective is considered met if average production rate is at least 125 anomalies / day.

3.6 OBJECTIVE: DATA THROUGHPUT

The collection of a complete, high-quality data set with the sensor platform is critical to the downstream success of the UXO Classification Study. This objective considers one of the key data quality issues, the ability of the data analysis workflow to support the data collection effort in a timely fashion. To maximize the efficient collection of high quality data, a series of MTADS standard data quality check are conducted during and immediately after data collection on site. Data which pass the QC screen are then processed into archival data stores. Individual anomaly analyses are then conducted on those archival data stores. The data QC / preprocessing portion of the workflow needs to keep pace with the data collection effort for best performance.

3.6.1 Metric

The throughput of the data quality control workflow is at least as fast the data collection process, providing real time feedback to the data collection team of any issues.

3.6.2 Data Requirements

The data analysts log books will provide the necessary data for determining the success of this metric.

3.6.3 Success Criteria

This objective is considered met if all collected data can be processed through the data quality control portion of the workflow in a timely fashion.

3.7 OBJECTIVE: RELIABILITY AND ROBUSTNESS

This objective represents an opportunity for all parties involved in the data collection process, especially the vehicle operator, to provide feedback on areas where the process could be improved.

3.7.1 Data Requirements

Discussions with, and/or observations by, the entire field team will allow for determining the success of this metric.

4.0 SITE DESCRIPTION

Please refer to the 2010 ESTCP UXO Classification Study Demonstration Plan.

5.0 TEST DESIGN

5.1 CONCEPTUAL EXPERIMENTAL DESIGN

The demonstration was executed in two stages during July 2010. The first stage was to characterize the TEMTADS sensor array being demonstrated with respect to the items of interest and to the site specific geology. On-site measurements, both in-air and on the IVS, were acquired for example articles of newly encountered items of interest; these have been supplemented with prior in-air measurements for those items of interest previously encountered. In addition, the background response of the demonstration site, as measured by the TEMTADS, was characterized throughout the data collection.

The second stage of the demonstration was a survey of the demonstration site using the TEMTADS array based on the anomaly list provided by the Program Office. The array was roughly centered over each anomaly position and a data set collected. Each data set was then inverted using the data analysis methodology discussed in Section 6.0, and the estimated target parameters determined. The fit results and the archive data were submitted to the Program Office along with this report.

5.2 SITE PREPARATION

Please refer to the 2010 ESTCP UXO Classification Study Demonstration Plan.

5.3 SYSTEMS SPECIFICATION

This demonstration was conducted using the NRL MTADS tow vehicle and subsystems. The tow vehicle and each subsystem are described further in the following sections.

5.3.1 MTADS Tow Vehicle

The MTADS has been developed with support from ESTCP. The MTADS hardware consists of a low-magnetic-signature vehicle that is used to tow the different sensor arrays over large areas (10 - 25 acres / day) to detect buried UXO. The MTADS tow vehicle and magnetometer array are shown in Figure 5-1.



Figure 5-1 – MTADS tow vehicle and magnetometer array.

5.3.2 RTK GPS System

Positioning is provided using cm-level Real Time Kinematic (RTK) Global Positioning System (GPS) receivers. To achieve cm-level precision, a fixed reference base station is placed on an established first-order survey control point near the survey area. The base station transmits corrections to the GPS rover at 1 Hz via a radio link (450 MHz). The TEMTADS array is located in three-dimensional space using a three-receiver RTK GPS system shown schematically in Figure 2-5 [10]. The three-receiver configuration extends the concept of RTK operations from that of a fixed base station and a moving rover to moving base stations and moving rovers. The lead GPS antenna (and receiver, Main) receives corrections from the fixed base station. This corrected position is reported at 10-20 Hz using a vendor-specific NMEA-0183 message format (PTNL,GGK or GGK). The Main receiver also operates as a ‘moving base,’ transmitting corrections (by serial cable) to the next GPS receiver (AVR1) which uses the corrections to operate in RTK mode.

A vector (AVR1, heading (yaw), angle (pitch), and range) between the two antennae is reported at 10 Hz using a vendor-specific NMEA-0183 message format (PTNL,AVR or AVR). AVR1 also provides ‘moving base’ corrections to the third GPS antenna (AVR2) and a second vector (AVR2) is reported at 10 Hz. All GPS measurements are recorded at full RTK precision, ~2-5 cm. For survey-mode arrays, all sensor readings are typically referenced to the GPS 1-PPS pulse output to fully take advantage of the precision of the GPS measurements. In this case of a cued survey, it is not necessary to address these timing issues. For the cued-mode survey, the GPS position is averaged for 2 seconds as part of the data acquisition cycle. The averaged position

and orientation information are then recorded to the position (.gps, ASCII format) data file. The details of the file format are provided in 0.

5.3.3 Time-Domain Electromagnetic Sensor

The TEMTADS array is a 5 x 5 square array of individual sensors. Each sensor has dimensions of 40 cm x 40 cm, for an array of 2 m x 2 m overall dimensions. The rationale of this array design is discussed in Reference 11. The result is a cross-track and down-track separation of 40 cm. The sensor array is mounted at a ride height of 17.5 cm above the ground. Sensor numbering is indicated in Figure 2-5. The transmitter electronics and the data acquisition computer are mounted in the tow vehicle. Custom software written by NRL provides both navigation to the individual anomalies and data acquisition functionality. After the array is positioned roughly centered over the center of the anomaly, the data acquisition cycle is initiated. Each transmitter is fired in a sequence winding outward clockwise from the center position (12). The received signal is recorded for all 25 Rx coils for each transmit cycle. The transmit pulse waveform duration is 2.7s (0.9s block time, 9 repeats within a block, 3 blocks stacked, with a 50% duty cycle). While it is possible to record the entire decay transient at 500 MHz, we have found that binning the data into 115 time gates simplifies the analysis and provides additional signal averaging without significant loss of temporal resolution in the transient decays as discussed in Section 2.1.1 [12]. The data are recorded in a binary format as a single file with 25 data points (one data point per Tx cycle). The filename corresponds to the anomaly ID from the target list under investigation.

5.4 CALIBRATION ACTIVITIES

A significant amount of TEMTADS data has been collected to date. Prior to the former Camp Butner demonstration, data was collected at our Blossom Point facility, both on a test stand and in the towed configuration over our test field [13], and during recent demonstrations at APG [6] and SLO [8]. These data provide us with a set of reference derived response coefficients for a variety of items, both UXO and clutter.

At the former Camp Butner demonstration, daily calibration efforts consisted of collecting background data sets at quiet spots periodically throughout the day. These quiet spots were deemed to be anomaly-free and, as a result, allowed us to gauge both the levels and spatial/temporal variations of the system noise at the site. The emplaced items in the IVS were also measured twice daily to monitor the variation in the system response to such items. Since these individual items were all newly encountered with no reference responses on hand to compare with, the variation was monitored by comparing the amplitudes of the derived response coefficients for each emplaced item to the running averages obtained throughout the demonstration.

A few in-air measurements of items of interest were also collected to supplement those data taken on the IVS and at earlier off-site locations. These data were submitted to the Program Office along with this report to provide additional training data to the classification demonstrators. An example of each munition-of-interest was available for precisely this purpose.

Please refer to the 2010 ESTCP UXO Classification Study Demonstration Plan for further details.

5.4.1 Background Data

A group of anomaly-free areas throughout the demonstration site were identified in advance using the EM61 data. The locations are listed in Table 5-1 and shown in Figure 5-2. These were all measured by the TEMTADS on the afternoon of the first day, the 5th of July, to determine their suitability as background candidates. Since they all roughly provided comparable responses, a convenient subset of these were chosen to be visited periodically throughout the day, on every day of the demonstration. All 122 background measurements taken for the duration of the demonstration (July 5-20) are shown in Figure 5-3, and are presented as the mean and standard deviation of the 25 monostatic measured signals. Table 5-2 offers details on the actual background areas visited each day, as well as the intraday variations of the mean and standard deviation quantities of Figure 5-3.

Table 5-1 – Locations of Anomaly-Free Areas used for Background Measurements.

ID	Easting (m)	Northing (m)
0	699393.6	4015891
1	699332.6	4015885
2	699341.6	4015881
3	699340.3	4015876
4	699392.5	4015866
5	699382.6	4015870
6	699377	4015866
7	699344.5	4015874
8	699312.1	4015847
9	699342	4015842
10	699366.8	4015735

The large intraday or diurnal variations that are visible especially during the second half of the demonstration interval were due to the ambient moisture conditions. The weather was hot and dry for most of the first week, except for a brief downpour in the early afternoon of July 10th, and then gradually became wetter over the remaining period as more (usually overnight) rain showers developed. The characteristic diurnal variation is one where the average measured signal, and the standard deviation, starts high early in the day (before the sun has had a chance to dry things off) and gradually settles to a more typical value. These typical values are also moisture dependent, as is most evident by the increasing average measured signal as the demonstration draws out in time, but nevertheless supported for the standard deviation as well through the entries in Table 5-2. The standard deviation of the 25 monostatic signals provides a relatively robust measure of the TEMTADS noise level which was seen to generally be in the 3.5-4 mV range at Camp Butner.

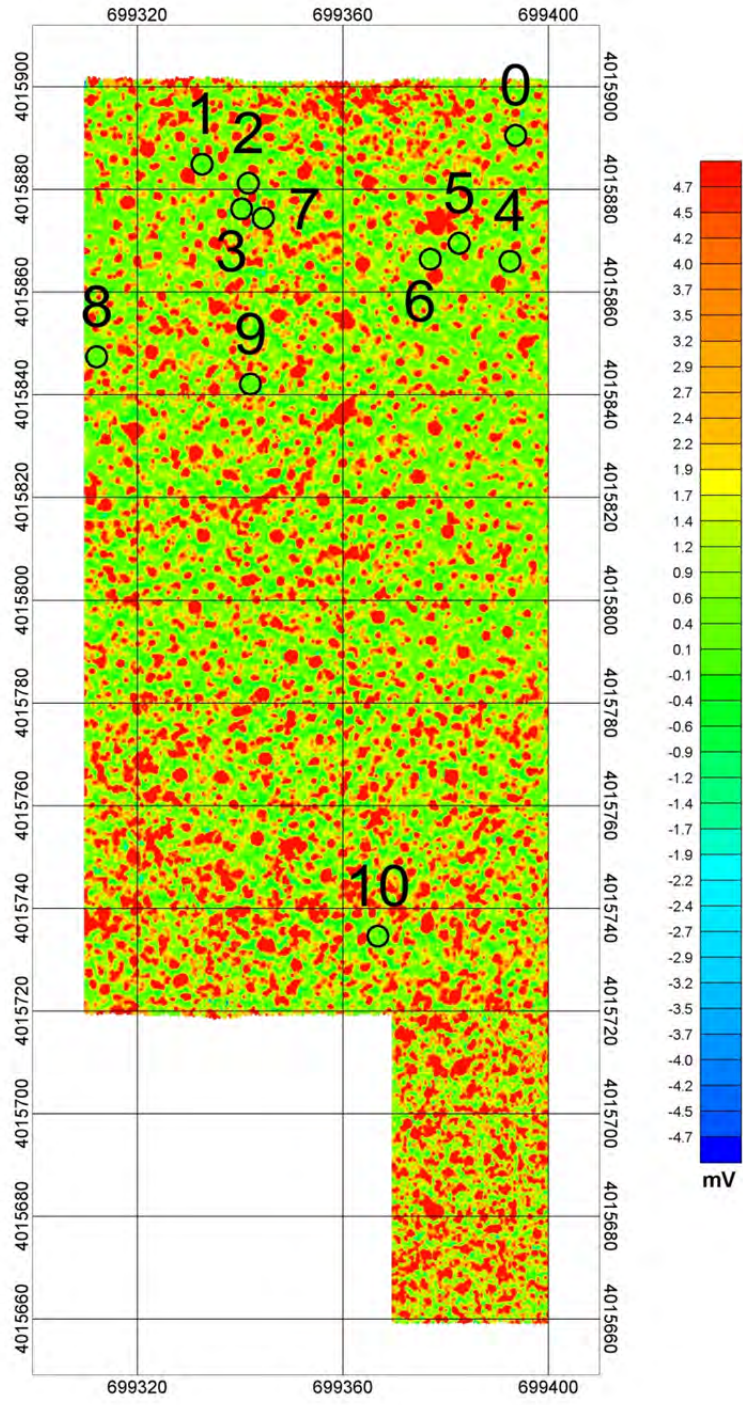


Figure 5-2 – Locations of anomaly-free areas determined beforehand from the EM61 cart data.

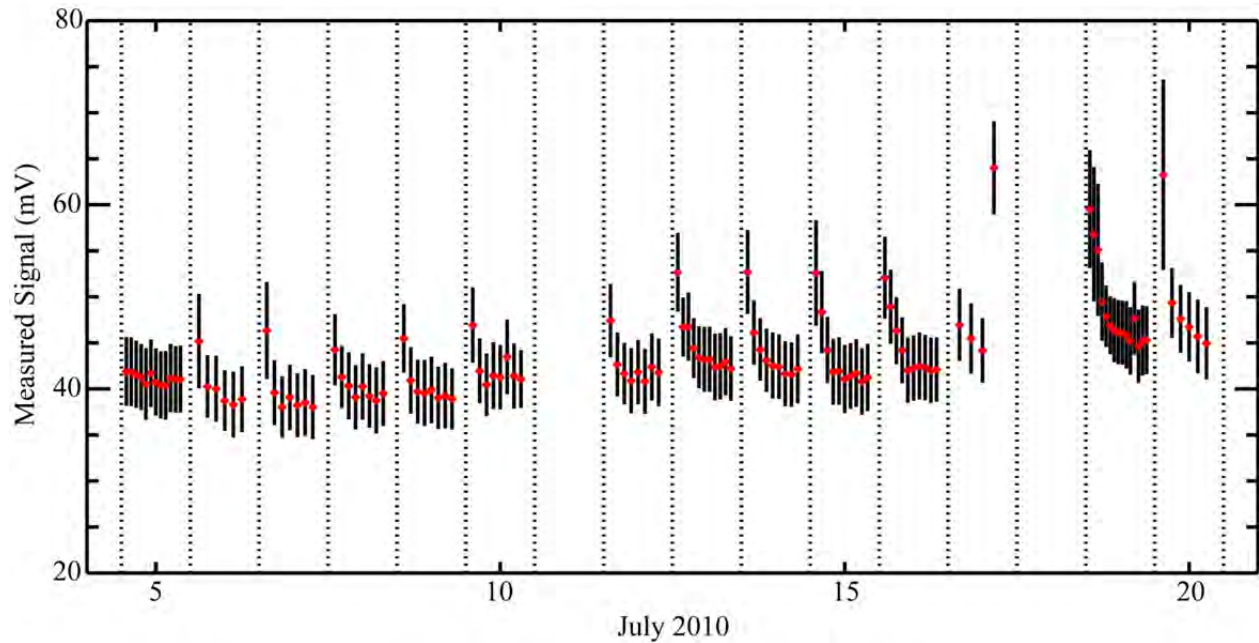


Figure 5-3 – Intra- and inter- daily variations in the response of the TEMTADS to background anomaly-free areas through the duration of the demonstration at Camp Butner. The red points represent the average measured signal of the 25 monostatic quantities, while the bars represent the standard deviation of those quantities (i.e. 1σ about the mean).

Table 5-2 – Summary of the Daily Variation in the Mean and Standard Deviation of the Signals Measured for the Background Areas.

Day	Background IDs	Total	Signal Mean (mV)		Signal σ (mV)	
			Mean	σ	Mean	σ
5	0(2),1,2,3,4,5,6,7,8,9,10	12	41.14	0.54	3.68	0.08
6	8(3),10(3)	6	40.23	2.55	3.75	0.68
7	8(3),10(4)	7	39.69	2.99	3.75	0.67
8	8(4),10(4)	8	40.34	1.78	3.57	0.15
9	8(3),10(5)	8	40.34	2.17	3.53	0.13
10	8(3),10(5)	8	42.25	2.08	3.60	0.32
12	0(2),8,10(5)	8	42.42	2.11	3.58	0.19
13	0(3),8(4),10(4)	11	44.59	3.12	3.56	0.28
14	0(3),10(6)	9	44.06	3.54	3.63	0.36
15	0(2),8,10(7)	10	43.52	3.91	3.92	0.69
16	0(2),8(2),10(6)	10	44.48	3.53	3.70	0.30
17	8,10(3)	4	50.15	9.31	4.08	0.69
19	0,8(10),10(4)	15	48.55	4.69	4.32	1.14
20	0(4),8,10	6	49.60	6.86	4.92	2.66

5.4.2 Instrument Verification Strip Data

The intention of the IVS was to provide the ability to verify system repeatability on several examples of items of interest. Details of the contents of the IVS are given in Table 5-3. Each emplaced item in the IVS was measured twice daily, once before starting the data collection process and a second time before shutting the system down at the end of each day.

Table 5-3 – Details of Former Camp Butner IVS

ID	Center_Northing	Center_Easting	Depth (m)	Type	Orientation
1001	4015784.925	699304.955	0.29	shotput	N/A
1002	4015790.080	699304.913	0.07	37mm projectile	Horizontal E/W
1003	4015795.108	699305.002	0.03	small ISO	Horizontal E/W
1004	4015799.957	699305.031	0.05	small ISO	Horizontal E/W
1005	4015804.943	699304.994	0.02	small ISO	Horizontal E/W
1006	4015809.982	699305.056	0.27	shotput	N/A

Although items similar to those emplaced in the IVS have previously been measured, enough differences existed when comparing the derived responses to the reference responses that a decision was made to monitor the system response variation by comparing the amplitudes of the derived response coefficients for each emplaced item to the running averages obtained throughout the demonstration. In addition to examining the system response variation, the IVS also allowed us to evaluate how well we could locate the emplaced items in terms of Easting, Northing and depth below ground level. All data sets for each of the emplaced IVS items were inverted using the data analysis methodology discussed in Section 6.0, and the estimated target parameters determined. We summarize the results in the following Figures and Tables.

Table 5-4 – Summary of the Amplitude Variations at 0.042 ms in the Derived Response Coefficients for All Items Emplaced in the IVS.

ID	β_1 Amplitude				β_2 Amplitude				β_3 Amplitude			
	Min	Max	Mean	RMS	Min	Max	Mean	RMS	Min	Max	Mean	RMS
1001	3.66	3.97	3.81	0.07	3.60	3.89	3.75	0.08	3.39	3.87	3.55	0.10
1002	0.59	0.68	0.62	0.02	0.29	0.35	0.31	0.01	0.27	0.31	0.29	0.01
1003	0.51	0.61	0.56	0.02	0.20	0.29	0.26	0.03	0.21	0.25	0.23	0.01
1004	0.49	0.56	0.53	0.02	0.19	0.29	0.27	0.03	0.21	0.28	0.26	0.01
1005	0.45	0.56	0.53	0.02	0.26	0.54	0.31	0.06	0.21	0.25	0.22	0.01
1006	4.43	4.85	4.68	0.11	4.21	4.56	4.41	0.08	3.91	4.54	4.15	0.12

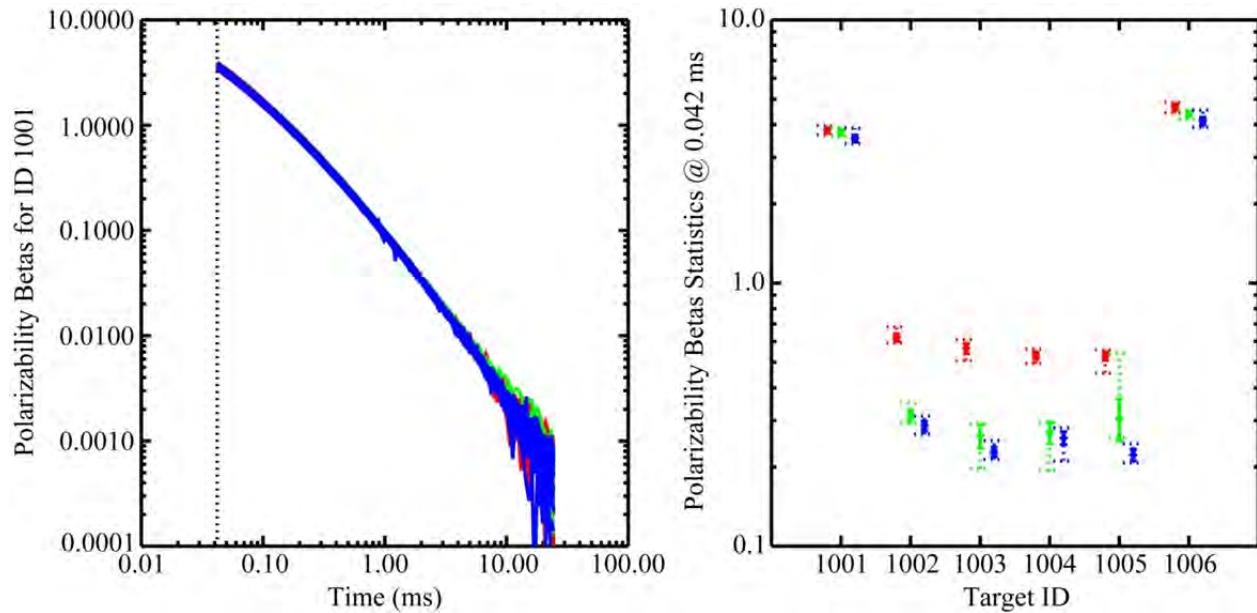


Figure 5-4 – Derived response coefficients for item 1001 emplaced in the IVS (left panel) and amplitude variations at 0.042 ms in the derived response coefficients for all items emplaced in the IVS (right panel). β_1 is in red; β_2 is in green; and β_3 is in blue.

The derived response coefficients (β_1 , β_2 , β_3) for all 23 data sets taken over item 1001 of the IVS over the duration of the demonstration are plotted in the left panel of Figure 5-4. As expected, the amplitudes of the three coefficients are comparable in amplitude suggesting a spherical shape. Furthermore, upon examining the variation in the amplitude at 0.042 ms in the decay, it is observed (from right panel, Figure 5-4 and first entry in Table 5-4) that the rms (σ) variation is less than 3% of the mean amplitude. Indeed, the observation can be made that apart from three cases for the β_2 coefficient (items 1003, 1004 and 1005), all rms variations fall below 5% of the respective mean amplitudes. Finally, it is important to note that for items 1002-1005 that except for one data set, all remaining 91 data sets point convincingly to a cylindrical shape where β_2 and β_3 are comparable and smaller than β_1 .

The Easting and Northing position errors for all 23 data sets taken over item 1001 of the IVS over the duration of the demonstration are plotted in the left panel of Figure 5-5. The position error is defined as the fit position (or, equivalently, the inverted position parameter) minus the ground truth position given in Table 5-3. In a perfect world, these errors would contain as many negative results as positive ones, with the mean position errors for each item being close to zero. As Figure 5-5 reveals, this is roughly true for the majority of emplaced items except for item 1001 which shows small but systematic biases in both the Easting and Northing position errors. In terms of the rms variation in inverted vs. reported positions for each emplaced IVS item, these were all under 1 cm, except for two cases (Northing errors for items 1001 and 1005) where the rms values approached 2 cm.

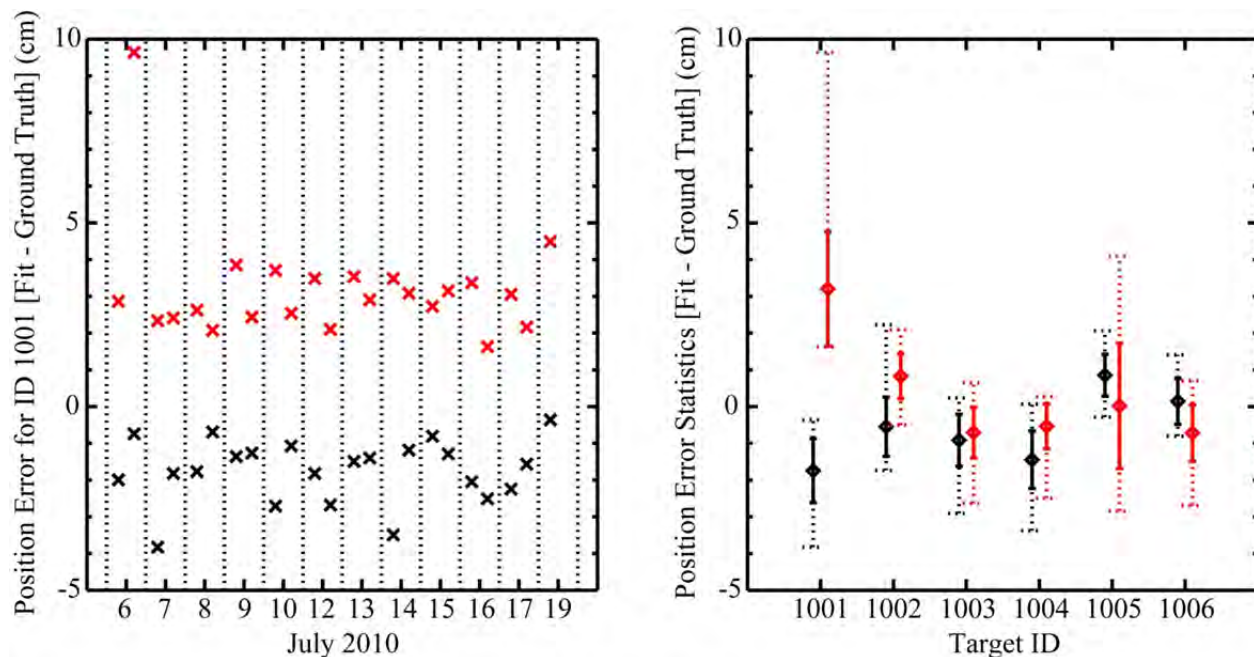


Figure 5-5 – Position errors for item 1001 emplaced in the IVS (left panel) and position error statistics for all items emplaced in the IVS (right panel). Easting data are in black and Northing data are in red.

Finally, it should be mentioned that the rms variation in inverted vs. reported depths for each emplaced IVS item were all comfortably below 1 cm. The statistics on depth error for each item are also provided in Table 5-5.

Table 5-5 – Summary of Position and Depth Error Statistics for all items emplaced in the IVS.

ID	Easting Position Error (cm)				Northing Position Error (cm)				Depth Error (cm)			
	Min	Max	Mean	RMS	Min	Max	Mean	RMS	Min	Max	Mean	RMS
1001	-3.8	-0.4	-1.7	0.9	1.6	9.6	3.2	1.6	-2.2	1.9	-1.2	0.8
1002	-1.7	2.2	-0.5	0.8	-0.5	2.1	0.8	0.6	0.8	2.8	1.9	0.5
1003	-2.9	0.2	-0.9	0.7	-2.6	0.6	-0.7	0.7	-2.0	1.0	-1.1	0.7
1004	-3.4	0.1	-1.4	0.8	-2.5	0.3	-0.5	0.6	-0.5	1.0	0.3	0.4
1005	-0.3	2.1	0.9	0.6	-2.8	4.1	0.0	1.7	-0.6	2.0	0.4	0.6
1006	-0.8	1.4	0.1	0.6	-2.7	0.7	-0.7	0.8	-2.0	0.8	-1.2	0.6

5.5 DATA COLLECTION PROCEDURES

5.5.1 Scale of Demonstration

A cued discrimination survey was conducted from July 5-20, 2010 within the 10 acre final demonstration site at the former Camp Butner, NC FUDS using the NRL TEMTADS. The anomaly list supplied by the ESTCP Program Office provided locations for the 2,304 anomalies identified from the EM61 MkII Cart data set. On-site measurements, both in-air and on the IVS,

were acquired for example articles of newly encountered items of interest; these have been supplemented with prior in-air measurements to account for those items of interest previously encountered. Each data set was inverted using the data analysis methodology discussed in Section 6.0, and the estimated target parameters determined. The fit results and the archive data were submitted to the Program Office along with this report.

5.5.2 Sample Density

The EMI data spacing for the TEMTADS is fixed at 40 cm in both directions by the array design.

5.5.3 Quality Checks

Preventative maintenance inspections were conducted at least once a day by all team members, focusing particularly on the tow vehicle and sensor trailer. Parts, tools, and materials for many maintenance scenarios are available in the system spares inventory which was on site. Status on any break-downs / failures which resulted in significant delays in operations was immediately reported to the ESTCP Program Office.

The TEMTADS data QC procedures and checks were as follows:

The status of the RTK GPS system was visually determined by the operator prior to starting the data collection cycle, assuring that the position and orientation information were valid, typical Fix Quality (FQ) 3, during the collection period. A Fix Quality (FQ) value of 3 (RTK Fixed) is the best accuracy (typically 3-5 cm or better). A FQ value of 2 (RTK Float) indicates that the highest level of RTK has not been reached yet and location accuracy can be degraded to as poor as ~1 m. FQs 1 & 4 correspond to the Autonomous and DGPS operational modes, respectively. Only data collected under FQ 3 were retained.

As an initial quick check on signal quality, contour plots of the background-subtracted signal were generated for the 25 transmit/receive pairs at a decay time of 0.042 ms. The plots were visually inspected to verify that there was a well-defined anomaly without unexplained extraneous signals or dropouts. An example of a good data set from a single well-isolated anomaly with a large SNR is shown in Figure 5-6. Since the contour plots do not reveal anything about the signal quality at later decay times or about the quality of the transmit/receive cross terms, a second and more thorough check was based on the dipole inversion results. Our experience has shown that data glitches show up as reduced dipole fit coherence.

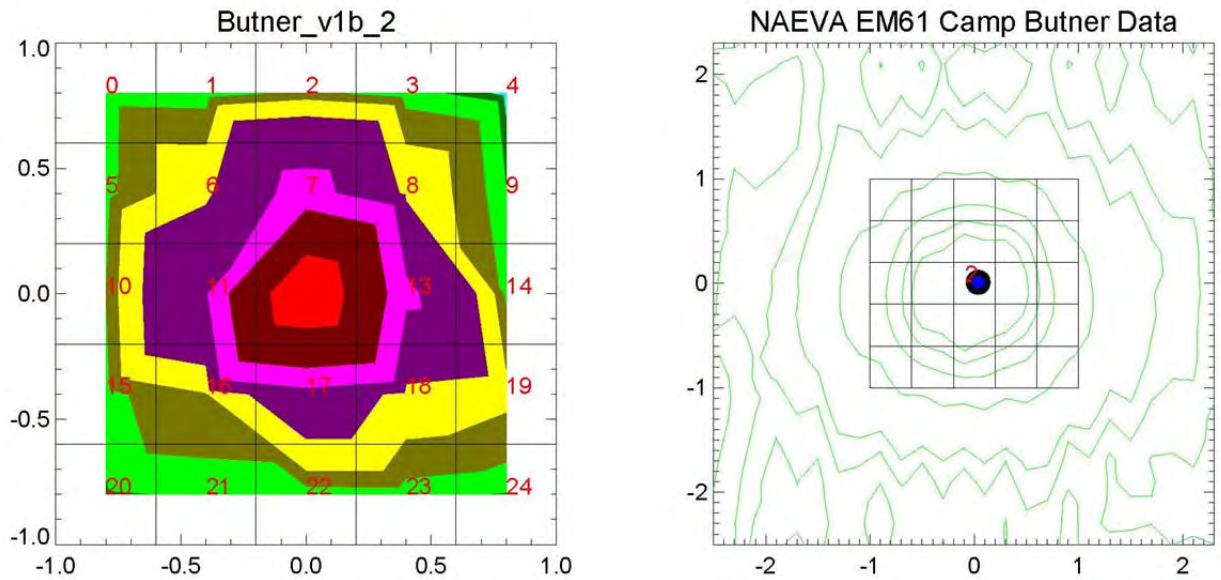


Figure 5-6 – QC tool showing a contour plot of the monostatic signals at 0.042 ms for the 25 transmit/receive pairs (left panel) alongside a contour plot of a 5 m x 5 m area of the EM61 data centered about the array and showing all the anomalies that are on the list and within this area (right panel).

Any data set that was deemed unsatisfactory by the data analyst was flagged and logged for future reacquisition. There were several reasons why the data set was deemed unsatisfactory. First, based on the contour plots, sometimes the peak believed to be the target, or a peak due to another nearby item, was off-center, such that our initial acquisition did not adequately capture the footprint. For such cases, updated anomaly coordinates were determined before reacquiring. Second, there were times when the data had a low SNR. The decision threshold for the vehicle operator for calling a measurement low SNR was a maximum signal amplitude of 5mV/A (background subtracted) for any monostatic term on the data acquisition display. For these cases, both reacquiring with increased stacking and reacquiring at two slightly offset (roughly 20cm) positions over the anomaly were initially tried and found to be comparable in effectiveness. Because the increased stacking was a much more time intensive process, the two position reacquisition mode became the standard for reacquiring low SNR data.

Data which meet the QC standards presented here are of the quality typical of the TEMTADS.

5.5.4 Data Handling

Data were stored electronically as collected on the MTADS vehicle data acquisition computer hard drives. Approximately every two survey hours, the collected data were copied onto removable media and transferred to the data analyst for QC/analysis. The data were moved onto the data analyst's computer and the media recycled. Raw data and analysis results were backed up from the data analyst's computer to optical media (CD-R or DVD-R) or external hard disks daily. These results were archived on an internal file server at NRL or SAIC at the end of the

survey. Examples of the TEMTADS file formats are provided in 0. All field notes / activity logs are written in ink and stored in archival laboratory notebooks. These notebooks are archived at NRL or SAIC. Relevant sections are reproduced in demonstration reports. Dr. Tom Bell is the POC for obtaining data and other information. His contact information is provided in Appendix A of this report.

5.6 VALIDATION

At the conclusion of data collection activities, all anomalies on the master anomaly list assembled by the Program Office will be excavated. Each item encountered will be identified, photographed, its depth measured, its location determined using cm-level GPS, and the item removed if possible. All non-hazardous items will be saved for later in-air measurements as appropriate. This ground truth information, once released, will be used to fully validate the objectives listed in Section 3.0

6.0 DATA ANALYSIS PLAN

6.1 PREPROCESSING

The TEMTADS array has 25 transmitters/receiver pairs. For each transmit pulse, we record the response at all of the receivers. Hence, for each target we have a $25 \times 25 \times N$ data array, where N is the number of recorded time gates. Normally we use 121 logarithmically spaced gates. In preprocessing, the recorded signals are normalized by the transmitter currents to account for any transmitter variations. We subtract 0.028 ms from the nominal gate times to account for time delay due to effects of the receive coil and electronics [14]. The delay was determined empirically by comparing measured responses for test spheres with theory. Measured responses include distortions due to transmitter ringing and related artifacts out to about 0.040 msec. Consequently we only include response beyond 0.040 ms in our analysis. This leaves 115 gates spaced logarithmically between 0.042 ms and 25 ms.

The background response is subtracted from each target measurement using data collected in a nearby target-free region. We will inter-compare all of the background measurements to evaluate background variability and identify outliers which may correspond to measurements over non-ferrous targets. We did not observe significant background variability at our Blossom Point test site, and were able to use blank ground measurements from 100 meters away for background subtraction on targets in the test field.

Geo-referencing of the array data is based on the GPS data, which gives the location of the center of the array and the orientation of the array. Sensor locations within the array are fixed by the array geometry. Dipole inversion of the array data (Section 6.2) determines target location in local array-based coordinates. This will be transformed to absolute coordinates using the array location and orientation determined from the corresponding GPS data.

6.2 PARAMETER ESTIMATION

The raw signature data from the TEMTADS Array reflect details of the sensor/target geometry as well as inherent EMI response characteristics of the targets themselves. In order to separate out the intrinsic target response properties from sensor/target geometry effects we invert the signature data to estimate principal axis magnetic polarizabilities for the targets. The TEMTADS data are inverted using the standard induced dipole response model wherein the effect of eddy currents set up in the target by the primary field is represented by a set of three orthogonal magnetic dipoles at the target location [15]. The measured signal is a linear function of the induced dipole moment \mathbf{m} , which can be expressed in terms of a time dependent polarizability tensor \mathbf{B} as

$$\mathbf{m} = \mathbf{UBU}^T \cdot \mathbf{H}_0$$

where \mathbf{U} is the transformation matrix between the physical coordinate directions and the principal axes of the target and \mathbf{H}_0 is the primary field strength at the target. The eigenvalues $\beta_i(t)$ of the polarizability tensor are the principal axis polarizabilities.

Given a set of measurements of the target response with varying geometries or "look angles" at the target, the data can be inverted to determine the (X, Y, Z) location of the target, the orientation of its principal axes (ψ , θ , ϕ), and the principal axis polarizabilities (β_1 , β_2 , β_3). The basic idea is to search out the set of nine parameters (X, Y, Z, ψ , θ , ϕ , β_1 , β_2 , β_3) that minimizes the difference between the measured responses and those calculated using the dipole response model.

For the TEMTADS array data, inversion is accomplished by a two-stage method. In the first stage, the target's (X, Y, Z) dipole location beneath is solved for non-linearly. At each iteration within this inversion, the nine element polarizability tensor (\mathbf{B}) is solved linearly. We require that this tensor be symmetric; therefore, only six elements are unique. Initial guesses for X and for Y are determined by a signal-weighted mean. The routine normally loops over a number of initial guesses in Z, keeping the result giving the best fit as measured by the chi-squared value. The non-linear inversion is done simultaneously over all time gates, such that the dipole (X, Y, Z) location applies to all decay times. At each time gate, the eigenvalues and angles are extracted from the polarizability tensor.

In the second stage, six parameters are used: the three spatial parameters (X, Y, Z) and three angles representing the yaw, pitch, and roll of the target (Euler angles ψ , θ , ϕ). Here the eigenvalues of the polarizability tensor are solved for linearly within the 6-parameter non-linear inversion. In this second stage both the target location and its orientation are required to remain constant over all time gates. The value of the best fit X, Y, and Z from the first stage, and the median value of the first-stage angles are used as an initial guess for this stage. Additional loops over depth and angles are included to better ensure finding the global minimum.

Figure 6-1 shows an example of the principal axis polarizabilities determined from TEMTADS array data. The target, a mortar fragment, is a slightly bent plate about ½ cm thick, 25 cm long, and 15 cm wide. The red curve is the polarizability when the primary field is normal to the surface of the plate, while the green and blue curves correspond to cases where the primary field is aligned along each of the edges.

Not every target on the target list will have a strong enough TEM response to support extraction of target polarizabilities. All of the data will be run through the inversion routines, and the results will be manually screened to identify those targets that cannot be reliably parameterized. Several criteria will be used in this process: signal strength relative to background, dipole fit error (difference between data and model fit to data), and the visual appearance of the polarizability curves.

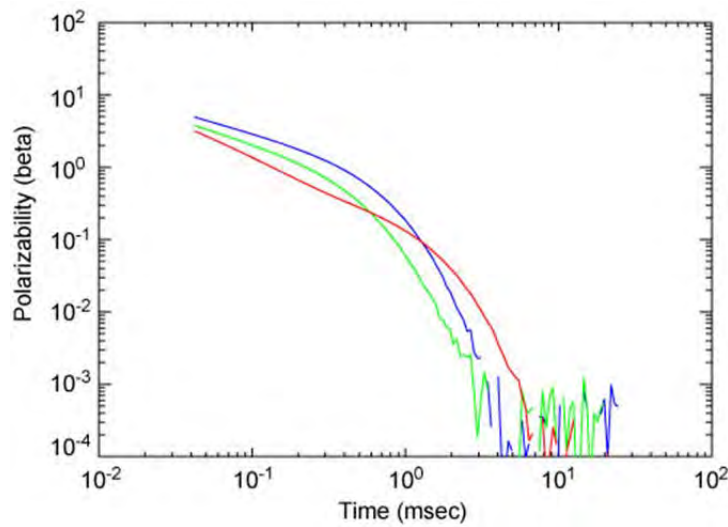


Figure 6-1 – Principal axis polarizabilities for a ½ cm thick by 25cm long by 15cm wide mortar fragment.

6.3 DATA PRODUCT SPECIFICATIONS

See 0 for the detailed data product specifications.

7.0 PERFORMANCE ASSESSMENT

The performance objectives for this demonstration were summarized in Table 3-1, and are repeated here as Table 7-1. The results for each criterion are then discussed in the following sections.

7.1 OBJECTIVE: SITE COVERAGE

A list of previously identified anomalies was provided by the Program Office.

7.1.1 Metric

Site coverage is defined as the fraction of the assigned anomalies surveyed by the TEMTADS.

7.1.2 Data Requirements

The collected data were compared to the original anomaly list. All interferences were noted in the field log book.

7.1.3 Success Criteria

The objective is considered met if 100% of the assigned anomalies are surveyed with the exception of areas that cannot be surveyed due to topology / vegetation interferences.

7.1.4 Results

This objective was successfully met. Of the list provided by the Program Office, all were measured.

7.2 OBJECTIVE: INSTRUMENT VERIFICATION STRIP RESULTS

This objective confirms that the sensor system is in good working order and collecting physically valid data each day. The IVS was surveyed twice daily. The amplitude of the derived response coefficients for each emplaced item is compared to the running average of the demonstration for reproducibility. The extracted fit location of each item is compared to the reported ground truth.

7.2.1 Metric

The reproducibility of the measured response of the sensor system to the emplaced items and of the extracted locations of the emplaced items defines this metric.

7.2.2 Data Requirements

The tabulated fit parameters for the data corresponding to each emplaced item in terms of derived response coefficients, location and depth.

Table 7-1 – Performance Results for this Demonstration.

Performance Objective	Metric	Data Required	Success Criteria	Success?
Quantitative Performance Objectives				
Site Coverage	Fraction of assigned anomalies interrogated	Survey results	100% as allowed for by topography / vegetation	Yes
Instrument Verification Strip (IVS) Results	System responds consistently to emplaced items	Daily IVS data	<ul style="list-style-type: none"> • $\leq 15\%$ rms variation in β amplitude • Down-track location $\pm 25\text{cm}$ 	<ul style="list-style-type: none"> • No • Yes
Location Accuracy	Average error and standard deviation in both axes for interrogated items	<ul style="list-style-type: none"> • Estimated location from IVS analyses • Ground truth from Table 5-3 	ΔN and $\Delta E < 5\text{ cm}$ σN and $\sigma E < 10\text{ cm}$	Yes
Depth Accuracy	Standard deviation in depth for interrogated items	<ul style="list-style-type: none"> • Estimated location from IVS analyses • Ground truth from Table 5-3 	$\Delta \text{Depth} < 5\text{ cm}$ $\sigma \text{Depth} < 10\text{ cm}$	Yes
Production Rate	Number of anomalies investigated each day	<ul style="list-style-type: none"> • Survey results • Log of field work 	125 anomalies/day	Yes
Data Throughput	Throughput of data QC process	Log of analysis work	All data QC'ed on site and at pace with survey	Yes
Qualitative Performance Objective				
Reliability and Robustness	General Observations	Team feedback and recording of emergent problems	Field team comes to work smiling	Yes

7.2.3 Success Criteria

The objective is considered met if the RMS amplitude variation of the derived response coefficients is less than 15% and the down-track fit location of the anomaly is within 25 cm of the stated location.

7.2.4 Results

As discussed in section 5.4.2, all but three cases (the β_2 response coefficient for items 1003, 1004 and 1005) had RMS amplitude variations that fell well below the 15% cutoff. The RMS amplitude variation for the β_2 coefficient (item 1005), however, exceeds 15% (refer to Table 5-4) and so this criterion is not met. Referring to Table 5-5, it is clear that the down-track fit location of the anomaly is well within 25 cm of the stated location, and so the second criterion is met.

7.3 OBJECTIVE: LOCATION ACCURACY

An important measure of how efficiently any required remediation will proceed is the accuracy of predicted location of the targets marked to be dug. Large location errors lead to confusion among the UXO technicians assigned to the remediation costing time and often leading to removal of a small, shallow object when a larger, deeper object was the intended target.

7.3.1 Metric

The average error and standard deviation in both horizontal axes defines this metric.

7.3.2 Data Requirements

The anomaly fit parameters and the ground truth for the excavated items. *Since these data are not available to us at this time, the IVS data are used to determine the performance of the fitting routines in terms of the location accuracy.*

7.3.3 Success Criteria

This objective is considered met if the average error in position for both Easting and Northing quantities is less than 5 cm and the standard deviation for both is less than 10 cm.

7.3.4 Results

Referring to Table 5-5, it is clear that the largest average error in either the Easting or Northing position is 3.2 cm and the largest standard deviation is even less. This means the location accuracy objective has been met.

7.4 OBJECTIVE: DEPTH ACCURACY

An important measure of how efficiently any required remediation will proceed is the accuracy of predicted depth of the targets marked to be dug. Large depth errors lead to confusion among the UXO technicians assigned to the remediation costing time and often leading to removal of a small, shallow object when a larger, deeper object was the intended target.

7.4.1 Metric

The standard deviation of the predicted depths with respect to the ground truth defines this metric.

7.4.2 Data Requirements

The anomaly fit parameters and the ground truth for the excavated items. *Since these data are not available to us at this time, the IVS data are used to determine the performance of the fitting routines in terms of the depth accuracy.*

7.4.3 Success Criteria

This objective is considered met if the average error in depth is less than 5 cm and the standard deviation is less than 10 cm.

7.4.4 Results

Referring to Table 5-5, it is clear that the largest average error in depth is 1.9 cm and the largest standard deviation is even less. This means the depth accuracy objective has been met.

7.5 OBJECTIVE: PRODUCTION RATE

This objective considers a major cost driver for the collection of high-density, high-quality geophysical data, the production rate. The faster quality data can be collected, the higher the financial return on the data collection effort.

7.5.1 Metric

The number of anomalies investigated per day determines the production rate for a cued survey system.

7.5.2 Data Requirements

The metric can be determined from the combination of the field logs and the survey results. The field logs require the amount of time per day spent acquiring the data and the survey results determine the number of anomalies investigated in that time period.

7.5.3 Success Criteria

This objective is considered met if average production rate is at least 125 anomalies / day.

7.5.4 Results

This objective was successfully met. A total of 2473 anomalies (including redos) were measured over a 13-day run for an average of 190 anomalies/day. The only days for which our average fell

below our goal of 125 anomalies/day were on July 17th when we had to shut down operations early due to persistent rain, and the final day when we were finishing up the redos.

7.6 OBJECTIVE: DATA THROUGHPUT

The collection of a complete, high-quality data set with the sensor platform is critical to the downstream success of the UXO Classification Study. This objective considers one of the key data quality issues, the ability of the data analysis workflow to support the data collection effort in a timely fashion. To maximize the efficient collection of high quality data, a series of MTADS standard data quality check are conducted during and immediately after data collection on site. Data which pass the QC screen are then processed into archival data stores. Individual anomaly analyses are then conducted on those archival data stores. The data QC / preprocessing portion of the workflow needs to keep pace with the data collection effort for best performance.

7.6.1 Metric

The throughput of the data quality control workflow is at least as fast the data collection process, providing real time feedback to the data collection team of any issues.

7.6.2 Data Requirements

The data analysts log books will provide the necessary data for determining the success of this metric.

7.6.3 Success Criteria

This objective is considered met if all collected data can be processed through the data quality control portion of the workflow in a timely fashion.

7.6.4 Success Criteria

This objective was successfully met. Data were normally downloaded several times during each workday, and quality control on these datasets was usually completed on the same day. Quality control checks successfully caught missed anomalies, a small number of corrupt data files, and targets which needed re-measuring.

7.7 OBJECTIVE: RELIABILITY AND ROBUSTNESS

This objective represents an opportunity for all parties involved in the data collection process, especially the vehicle operator, to provide feedback on areas where the process could be improved.

7.7.1 Data Requirements

Discussions with, and/or observations by, the entire field team will allow for determining the success of this metric.

7.7.2 Results

This objective was successfully met. Based on vehicle operator feedback, there were no significant limitations to the efficient use of the system in the field.

8.0 REFERENCES

1. “2010 ESTCP Classification Study, Former Camp Butner, NC, May 2010,” Draft 6, ESTCP Program Office, August 9, 2010.
2. “MTADS Demonstration at Camp Sibert Magnetometer / EM61 MkII / GEM-3 Arrays,” Demonstration Data Report, G.R. Harbaugh, D.A. Steinhurst, N. Khadr, August 21, 2008.
3. “Enhanced UXO Discrimination Using Frequency-Domain Electromagnetic Induction,” ESTCP MR-0033 Final Report, June 27, 2007.
4. “Survey of Munitions Response Technologies,” ESTCP, ITRC, and SERDP, June, 2006.
5. “ESTCP MR-0744, Demonstration Data Report, Former Camp San Luis Obispo, Magnetometer and EM61 MkII Surveys,” G.R. Harbaugh, N. Khadr, and D.A. Steinhurst, accepted May 7, 2010.
6. “STANDARDIZED UXO TECHNOLOGY DEMONSTRATION SITE SCORING RECORD NO. 920 (NRL),” J.S. McClung, ATC-9843, Aberdeen Test Center, MD, November, 2008.
7. “EMI Array for Cued UXO Discrimination, ESTCP MR-0601, Demonstration Data Report, APG Standardized UXO Test Site,” G.R. Harbaugh, J.B. Kingdon, T. Furuya, T.H. Bell, and D.A. Steinhurst, Naval Research Laboratory Memorandum Report NRL/MR/6110—00-9234, January 14, 2010.
8. “ESTCP MR-0744, Demonstration Data Report, Former Camp San Luis Obispo, TEMTADS Cued Survey,” G.R. Harbaugh, D.A. Steinhurst, D.C. George, J.B. Kingdon, D.A. Keiswetter, and T.H. Bell, accepted May 7, 2010.
9. “EMI Array for Cued UXO Discrimination, ESTCP MR-0601, Final Report,” D.C. George, J.B. Kingdon, T. Furuya, D.A. Keiswetter, T.H. Bell G.R. Harbaugh, and D.A. Steinhurst, Naval Research Laboratory Memorandum Report NRL/MR/6110—00-9289, September 16, 2010.
10. Steinhurst, D., Khadr, N., Barrow, B., and Nelson, H. “Moving Platform Orientation for an Unexploded Ordnance Discrimination System,” GPS World, 2005, 16/5, 28 – 34.
11. Nelson, H. H., “Array Specification Report,” ESTCP Project MR-0601, June, 2007.
12. Nelson, H. H., ESTCP In-Progress Review, ESTCP Project MR-0601, March 1, 2007.

13. Nelson, H. H. and Robertson, R., "Design and Construction of the NRL Baseline Ordnance Classification Test Site at Blossom Point," Naval Research Laboratory Memorandum Report NRL/MR/6110—00-8437, March 20, 2000.
14. Bell, T., Barrow, B., Miller, J., and Keiswetter, D., "Time and Frequency Domain Electromagnetic Induction Signatures of Unexploded Ordnance," *Subsurface Sensing Technologies and Applications* Vol. 2, No. 3, July 2001.
15. Bell, T. H., Barrow, B. J., and Miller, J. T., "Subsurface Discrimination Using Electromagnetic Induction Sensors," *IEEE Transactions on Geoscience and Remote Sensing*, Vol. 39, No. 6, June 2001.

APPENDIX A. POINTS OF CONTACT

POINT OF CONTACT	ORGANIZATION	Phone Fax e-mail	Role in Project
Dr. Jeff Marqusee	ESTCP Program Office 901 North Stuart Street, Suite 303 Arlington, VA 22203	703-696-2120 (V) 703-696-2114 (F) jeffrey.marqusee@osd.mil	Director, ESTCP
Dr. Anne Andrews	ESTCP Program Office 901 North Stuart Street, Suite 303 Arlington, VA 22203	703-696-3826 (V) 703-696-2114 (F) anne.andrews@osd.mil	Deputy Director, ESTCP
Dr. Herb Nelson	ESTCP Program Office 901 North Stuart Street, Suite 303 Arlington, VA 22203	703-696-8726 (V) 703-696-2114 (F) 202-215-4844 (C) herbert.nelson@osd.mil	Program Manager, MM
Ms. Katherine Kaye	HydroGeoLogic, Inc. 11107 Sunset Hills Road, Suite 400 Reston, VA 20190	410-884-4447 (V) kkaye@hgl.com	Program Manager Assistant, MM
Mr. Daniel Reudy	HydroGeoLogic, Inc. 11107 Sunset Hills Road, Suite 400 Reston, VA 20190	703-736-4531 (V) druedy@hgl.com	Program Manager's Assistant, MM
Dr. Dan Steinhurst	Nova Research, Inc. 1900 Elkin St., Ste. 230 Alexandria, VA 22308	202-767-3556 (V) 202-404-8119 (F) 703-850-5217 (C) dan.steinhurst@nrl.navy.mil	PI
Mr. Glenn Harbaugh	Nova Research, Inc. 1900 Elkin St., Ste. 230 Alexandria, VA 22308	301-392-1702 (V) 804-761-5904 (C) glenn.harbaugh.ctr@nrl.navy.mil	Site Safety Officer
Dr. Tom Bell	SAIC 1225 S. Clark Street Suite 800 Arlington, VA 22202	(703)-414-3904 (V) thomas.h.bell@saic.com	Quality Assurance Officer

APPENDIX B. DATA FORMATS

B.1 POSITION / ORIENTATION DATA FILE (*.GPS)

```
Antenna,X_Offset,Y_Offset,Z_Offset,Easting/Yaw,Northing/Pitch,HAE/Range
Main,0.000,1.365,0.730,316256.990,4254211.094,-25.934
AVR1,-0.778,-1.418,0.740,3.40349,0.00761,2.882
AVR2,0.778,-1.418,0.745,1.55718,0.00425,1.554
```

These data files are ASCII format, comma-delimited files. A header line is provided.

Line 1 – Header information

Line 2 – Main GPS antenna data

Main	- Antenna Identifier
0.000	- Cross-track distance from array center
1.365	- Down-track distance from array center
0.730	- Vertical distance from array center
316256.990	- Easting (UTM, m) position of Main antenna
4254211.094	- Northing (UTM, m) position of Main antenna
-25.934	- Height-above-ellipsoid (m) position of Main antenna

Line 3 & 4 – AVR GPS antenna data (AVR1 as example)

AVR1	- Antenna Identifier
-0.778	- Cross-track distance from array center
-1.418	- Down-track distance from array center
0.740	- Vertical distance from array center
3.40349	- Yaw of AVR vector (radians, Grid North referenced)
0.00761	- Pitch of AVR vector (radians)
2.882	- Range of AVR vector (m)

B.2 TEM DATA FILE (*.TEM)

These data files are a binary format generated by a custom .NET serialization routine. They are converted to an ASCII, comma-delimited format in batches as required. Each file contains 25 data points, one data point corresponding to each Tx cycle. Each data point contains the Tx transient and the corresponding 25 Rx transients as a function of time. A pair of header lines is also provided for, one overall file header and one header per data point with the data acquisition parameters. A partial example is provided below.

Line 1 - File Header

```
CPUms,PtNo,LineNo,Delt,BlockT,nRepeats,DtyCyc,nStk,AcqMode,GateWid,Gate
HOff,TxSeq,GateT,TxI_Z,Rx0Z_TxZ,Rx1Z_TxZ,Rx2Z_TxZ,Rx3Z_TxZ,Rx4Z_TxZ,Rx5
Z_TxZ,Rx6Z_TxZ,Rx7Z_TxZ,Rx8Z_TxZ,Rx9Z_TxZ,Rx10Z_TxZ,Rx11Z_TxZ,Rx12Z_TxZ
,Rx13Z_TxZ,Rx14Z_TxZ,Rx15Z_TxZ,Rx16Z_TxZ,Rx17Z_TxZ,Rx18Z_TxZ,Rx19Z_TxZ,
Rx20Z_TxZ,Rx21Z_TxZ,Rx22Z_TxZ,Rx23Z_TxZ,Rx24Z_TxZ,
```

Line 2 - Data Point Header

```
0,1,0,2E-06,0.9,9,0.5,3,2,0.05,5E-05,22,  
0          - Start time in ms on CPU clock (always 0)  
1          - Data Point Number (always 1)  
0          - Line Number (always 0)  
2E-06     - Time step for transients (seconds)  
0.9       - Base period length (seconds)  
9         - Number of Tx cycles in a base period  
0.5       - Duty cycle  
3         - Number of base periods averaged (or stacked)  
2         - Data Acquisition Mode (binned)  
0.05      - Gate width as fraction of its own time  
5E-05     - Hold-off time (seconds) for first data point  
22        - Tx ID number (sensor number + 10)
```

Line 3 - First Data Line in First Data Point

```
,,,,,,,,,,,,,2.5E-05,2.01102465120852,-4.71949940100108E-05,-  
1.79793904939509E-05,1.39366551389817E-05,-2.55470612811271E-05,-  
4.84779418501355E-05,4.05641650778409E-05,6.73185201421361E-06,-  
0.000116516308079121,-2.49295973312366E-06,4.21216420108736E-  
05,3.70976690069955E-05,-0.000127606649206979,-0.000510366345393333,-  
0.000100251591870083,5.19149917311475E-05,3.71239440686929E-05,-  
6.05368361143584E-06,-0.000125671808025774,2.44747669528873E-  
05,5.7401043406257E-05,-5.14479298585597E-05,-9.42595187481444E-  
06,3.27817636140336E-05,-1.1886747308274E-05,-5.57022247620241E-05,
```

B.3 ANOMALY PARAMETER OUTPUT FILE

The MTADS DAS will be used to analyze TEMTADS data. The fitted parameters for each investigated anomaly are distributed as an Excel 2003 spreadsheet, but an excerpt is given in .csv format below for reference purposes. A header line is provided for information followed by a 116-line block for each anomaly. The first line of each block contains the time gate-independent fit parameters and the remaining 115 contain the time gate-dependent parameters for each anomaly.

```
Anomaly_ID,Anomaly_X,Anomaly_Y,Anomaly_Amplitude,Fit_X,Fit_Y,Fit_Depth(  
m),Fit_Phi(deg),Fit_Theta(deg),Fit_Psi(deg),Fit_Coherence,Time_Gate,Bet  
a1,Beta2,Beta3
```

```
28,402751.00,4369521.75,234.34,402750.926,4369521.686,0.151,250.42,2.02  
,76.57,0.99612,,,,,  
,,,,,,,,,,,,,1,1.47E+00,1.05E+00,1.08E+00  
.....  
.....  
.....  
.....  
115,2.46E-05,-1.69E-05,-1.60E-04  
  
33,402726.00,4369505.50,15.24,402725.835,4369505.588,0.422,96.25,16.45,  
5.26,0.96448,,,,,  
,,,,,,,,,,,,,1,1.71E+00,1.23E+00,1.18E+00  
.....
```

```
.....  
.....  
.....,115,6.56E-04,-1.91E-03,-1.57E-04
```

B.4 README FILE

The distributed data are also accompanied by an explanatory readme.txt file which is reproduced here for completeness:

There are 2 types of files included here. GPS files have the ".gps" suffix. They are described in Appendix C of the TEMTADS Demo Plan and Appendix B of the Demonstration Data Report. Files containing "_data" in their name are the TEMTADS measurements. These have been background-subtracted, and the signal from each transmitter has been divided by the peak current in that transmitter. Both the data files and beta files are further subdivided between the daily IVS measurements and the actual anomalies.

It will be noted that several files have multiple versions. These are the results of several factors: (1) Redos; (2) Increased stacking (averaging); (3) Two positions over the same anomaly; and (4) On the spot redos. We will discuss each of these below.

(1) Redos: For approximately 10% of the anomalies, either the peak believed to be the target, or a peak due to another object present within the anomaly were off-center, such that our initial acquisition did not adequately capture the footprint. New coordinates were determined, and the anomalies were remeasured. All such redos have an "r" appended to the anomaly number. For a small subset of these cases, more than one peak of interest was off-center, and two shots were taken. The second redo in such cases has "ra" appended. For example, in the original shot of anomaly 2087, 2 separate peaks were seen which were both off center. The original shot is called 2087, and the 2 redos are called 2087r and 2087ra.

(2) Increased stacking: Two experiments were performed to improve the classification of low SNR targets, increased stacking and taking two positions over the same anomaly. For targets below a set SNR value, which is determined after the initial acquisition, a second acquisition was performed with increased stacking. This should effectively increase our SNR by a factor of 2. Such cases have "_stacked" appended after the anomaly number. After a few days, our analysis indicated that the benefit gained by this was minimal compared with the extra time incurred. All targets that were given extra stacking were also done with 2 positions, as discussed below. Note that there are not separate .gps files for these stacked cases, since the position is identical to the original shot. The GPS files for the initial shot should be used. For example, for 2054_stack, use the GPS file for 2054.

(3) Two positions over the same anomaly: This is the second experiment conducted to try to improve the classification of low SNR targets. After the original acquisition, the array is moved forward slightly (roughly 20cm), and a second shot is taken. The idea here is that using the GPS data, the two datasets can be combined, and solved

simultaneously. Alternately, one can simply use both shots individually. In most cases, the second shot has an "a" appended to the anomaly number. Some confusion arises, however, with the next category.

(4) On the spot redos: On a small number of occasions, the operator felt that something was wrong with the initial measurement (poor GPS values, vehicle accidentally moved), and performed an immediate redo. The data acquisition software also appends an "a" to the anomaly number in these cases, creating confusion with the previous category. The operator erred on the side of caution in deciding to do these redos, and in many cases, the original shot may still be good. Therefore, with the exception of the most egregious cases, we have also included the original shot in this dataset.

There were also a relatively small number of targets that are somewhat of a cross between categories (1) and (4). These were cases where the redo was the result of water saturated ground, and so were done at approximately the same location as the original, but were done of necessity at a later time. These also have "a" appended.

The confusion noted above between categories (3) and (4) is of no concern unless the analyst wishes to perform a simultaneous inversion of the 2 positions, We therefore provide clarification on all such cases below:

455a - On the spot redo of 455
534a - On the spot redo of 534
862a - On the spot redo of 862
941a - Redo of 941 due to rain effects
1259b - Redo of 1259 and 1259a due to rain effects
1325a - 2nd position for 1325
1472a - Redo of 1472 due to rain effects
1512a - Redo of 1512 due to rain effects
1633a - Redo of 1633 due to rain effects
1662a - 2nd position for 1662
1712a - 2nd position for 1712
1779a - 2nd position for 1779
1806a - 2nd position for 1806
1819a - 2nd position for 1819
1830a - 2nd position for 1830
1867a - 2nd position for 1867
2023a - 2nd position for 2023
2035a - Redo of 2035 due to rain effects
2054a - 2nd position for 2054
2056a - Redo of 2056 due to rain effects
2063a - 2nd position for 2063
2109a - Redo of 2109 due to rain effects
2260a - Redo of 2260 due to rain effects
2325a - Redo of 2325 due to rain effects
2331a - 2nd position for 2331
2482a - 2nd position for 2482
2499a - 2nd position for 2499
2539a - Redo of 2539 due to rain effects
2552a - 2nd position for 2552
2616a - 2nd position for 2616
2624a - 2nd position for 2624
2700a - 2nd position for 2700

2748a - 2nd position for 2748
2816a - 2nd position for 2816
2823a - 2nd position for 2823
2825a - 2nd position for 2825
2900a - 2nd position for 2900
2904a - 2nd position for 2904
2931a - 2nd position for 2931
2935a - 2nd position for 2935
2939a - 2nd position for 2939
2941a - Redo of 2941 due to rain effects
3007a - 2nd position for 3007
3010a - 2nd position for 3010
3011a - Redo of 3011 due to rain effects
3043a - Redo of 3043 due to rain effects
3056c - Redo of 3056, 3056a, and 3056b due to rain effects
3088a - Redo of 3088 due to rain effects
3101a - 2nd position for 3101
3102a - 2nd position for 3102
3115a - 2nd position for 3115
3117a - 2nd position for 3117
3120a - 2nd position for 3120
3131a - 2nd position for 3131
3141a - 2nd position for 3141
3175a - Redo of 3175 due to rain effects
3190a - 2nd position for 3190
3200a - 2nd position for 3200
3207a - 2nd position for 3207
3220a - 2nd position for 3220
3246a - 2nd position for 3246
3257a - 2nd position for 3257
3261a - 2nd position for 3261
3277a - 2nd position for 3277
3283a - 2nd position for 3283
3334a - 2nd position for 3334
3337a - 2nd position for 3337
3339a - 2nd position for 3339
3345a - 2nd position for 3345
3362a - 2nd position for 3362
3377a - 2nd position for 3377
3396a - 2nd position for 3396
3399a - 2nd position for 3399
3409a - 2nd position for 3409
3428a - 2nd position for 3428
3450a - 2nd position for 3450
3453a - 2nd position for 3453
3479a - 2nd position for 3479
3503a - 2nd position for 3503
3510a - 2nd position for 3510
3521a - 2nd position for 3521
3527a - 2nd position for 3527
3550a - 2nd position for 3550
3554a - 2nd position for 3554
3573b - 2nd position for 3573a (3573a was a redo of 3573 due to rain effects)
3601a - 2nd position for 3601
3607a - 2nd position for 3607
3634a - 2nd position for 3634

3664a - 2nd position for 3664
3670a - 2nd position for 3670
3691a - 2nd position for 3691
3694a - 2nd position for 3694
3701a - 2nd position for 3701
3719a - 2nd position for 3719
3743a - 2nd position for 3743
3747a - 2nd position for 3747
3772a - 2nd position for 3772
3783a - 2nd position for 3783
3786a - 2nd position for 3786
3801a - 2nd position for 3801
3803a - Redo of 3803 due to rain effects
3816a - 2nd position for 3816
3824a - Redo of 3824 due to rain effects
3832a - 2nd position for 3832
3835a - Redo of 3835 due to rain effects
3837a - 2nd position for 3837
3839a - 2nd position for 3839
3846a - 2nd position for 3846
3874a - 2nd position for 3874
3888a - 2nd position for 3888
3898a - 2nd position for 3898
3905a - 2nd position for 3905
3910a - 2nd position for 3910